15th Prague Colloquium on *f*-Electron Systems

PCFES

PRAGUE COLLOQUIUM ON F-ELECTRON SYSTEMS

Prague, 17th - 20th June 2025

Program & Abstracts

Welcome to PCFES!

Almost every second year since 1992 we organized the *Prague Colloquium on f-Electron Systems*, an exciting meeting covering topics in physics of actinides and lanthanides. Also this year we keep the tradition having the pleasure to welcome you at 15th PCFES, an informal forum for presentations and discussions on the current issues of magnetism, strongly correlated systems, spectroscopies, materials science, as well as progress in theory. The meeting should also provide ground for close interaction of students and other early-stage researchers with experienced specialists.

Regarding the venue for PCFES, the Faculty of Mathematics and Physics belongs to the youngest faculties of the Charles University, which was founded in 1348 by the Roman Emperor and King of Bohemia, Charles IV. The Faculty itself was founded in 1952, splitting from the Faculty of Science. The building Ke Karlovu 5, where the PCFES sessions will take place, is now over 100 years old. Careful reconstructions succeeded to provide high functionality while meticulously preserving or restoring most of the details, carrying the spirit of the founders in early 1900s as well as following generations of professors and students. Part of the laboratories of the Department of Condensed Matter Physics (technology, X-ray diffraction, high-pressure lab) is located on the ground floor of the building. Neighbour building in the Ke Karlovu street, number 3, is the official and administrative seat of the Faculty. It is followed by the Church of the Virgin Mary and St. Charlemagne, built in the 14th century and known for its unique vaulted central dome without any support.

Down the street, the redbrick Maternity hospital and even farther the Psychiatric hospital (with the Antonin Dvorak museum opposite in a cute small baroque palace) complete the list of useful addresses.

The 15th Prague Colloquium on f-Electron Systems takes place with the contribution of material and human potential of the Department of Condensed Matter Physics, Faculty of Mathematics and Physics, Charles University.

Please feel comfortable in Prague, we wish you most enjoyable and productive days.

Silvie Mašková-Černá & Štěpán Sechovský
On behalf of the PCFES Organizers

USEFUL INFORMATION

Poster session

Besides the oral sessions, taking place in the lecture room F1, the discussions at posters will be possible on the 1st floor corridor. Presenters are requested to mount the posters as soon as possible and keep them for the whole duration of PCFES to allow informal discussions. One dedicated poster session will take place on Wednesday evening, during which presenters are expected to be present at their posters.

Refreshment

During PCFES, refreshment will be provided during coffee breaks and evenings. Lunches are not provided. You can find numerous small restaurants in the lively part of the town north of the Ke Karlovu street.

On-site connection to internet

It is possible to connect using Wi-Fi via **EDUROAM**.
Or
Special conference wifi access:
Please submit your MAC address via form on:
https://pcfes.kfkl.cz/wifi-connection-request/
Consequently, you will receive the connection SSID and password.

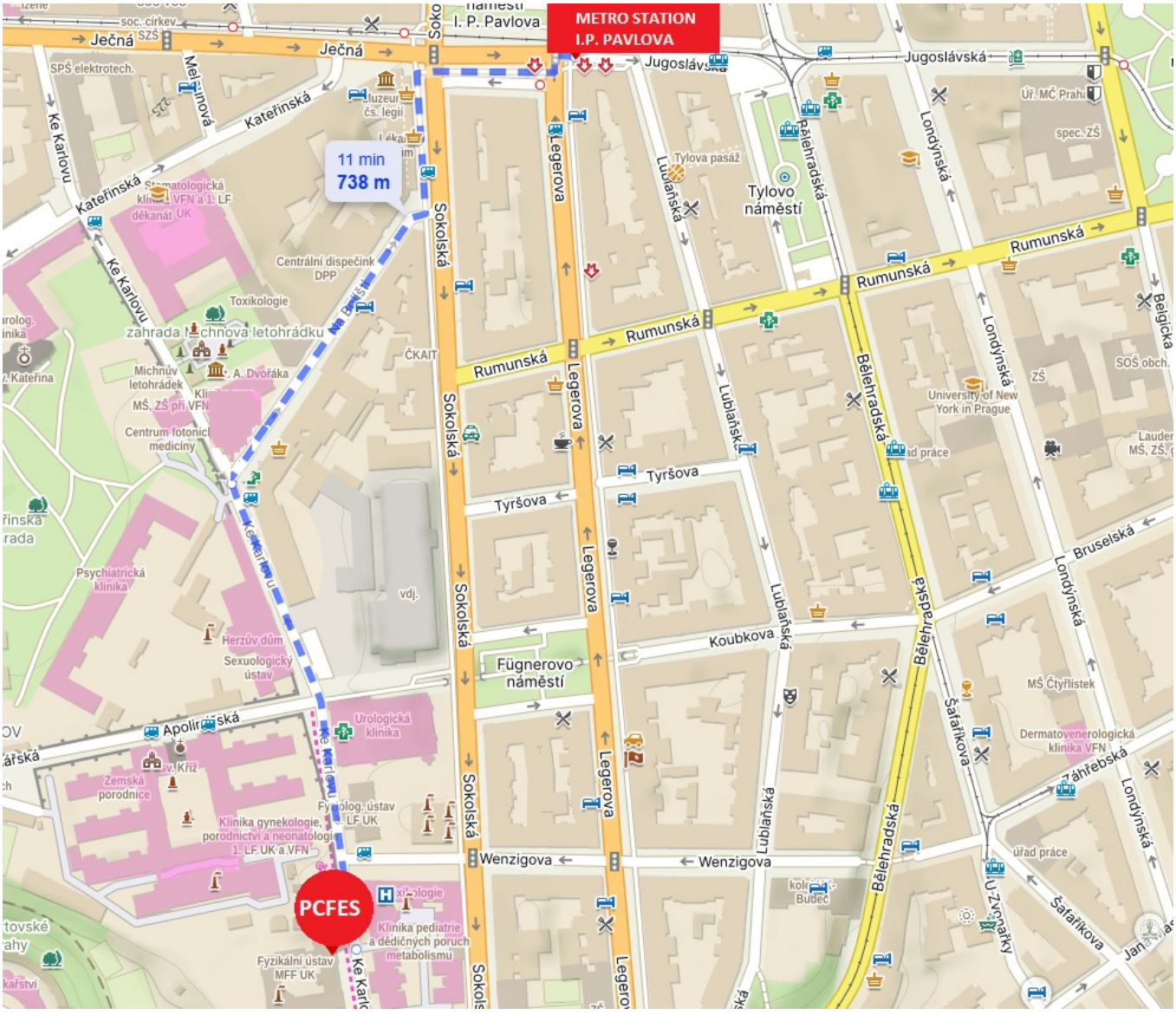

PROGRAM

Tuesday 17.06.2025			
	08:00	Registration	
	08:55	Opening	
	Spectroscopy I		
O01	09:00	James Tobin	**TUTORIAL** - HERFD vs XAS: The Case for Equivalence
O02	10:00	Denis Vyalikh	4*f*-driven surface effects in lanthanide materials from ARPES and XAS: Reorientation of 4*f* moments, 2D ferromagnetism, Kondo and Rashba effects
	10:30	***Coffee break***	
	Spectroscopy II		
O03	11:00	Jindřich Kolorenč	Can the Valence-to-Core RIXS Measured at the Uranium M5 Edge Quantify the Uranium–Ligand Hybridization in Insulators like UO_2 and UF_4?
O04	11:30	Ladislav Havela	XAS studies of U hydrides and other U systems - a key to the 5*f* occupancy?
	12:00	***Lunch***	
	Arsenides		
O05	14:00	Eteri Svanidze	Revisiting arsenides – from simple to complex
O06	14:30	Mitja Krnel	A new family of topological insulators RAsS (R = Y, La, Sm)
O07	15:00	Nazar Zaremba	New uranium-cobalt-arsenides with antiferromagnetic ordering
	15:30	***Coffee break***	
	RE-compounds I ($YbRh_2Si_2$)		
O08	16:00	Petra Knappová	Magnetic Susceptibility of $YbRh_2Si_2$
O09	16:30	Jan Knapp	The Heavy Fermion $YbRh_2Si_2$ – Spin Triplet Superconductor Underpinned by Antiferromagnetism
	17:00	***Welcome party***	

Wednesday 18.06.2025			
	Superconductivity		
O10	09:00	Oksana Karychort	New heavy fermion compound $Ce_6Rh_{30}As_{19}$: crystal structure and physical properties
O11	09:30	Anamaria Ghihor	Hybrid Superconducting Devices
O12	10:00	Özlem Evren	Synthesis and superconductivity of Be-based compounds
	10:30	***Coffee break***	
	Electronic structure – Theory I		
O13	11:00	Jeremy Sourd	Acoustic signatures of the field-induced electronic-topological transitions in $YbNi_4P_2$
O14	11:30	Ryszard Radwanski	Strongly electron-correlated atomic-like approach to 3d/4f/5f/4d/5d/ compounds
	12:00	***Lunch***	
	Complex behavior		
O15	14:00	Phillip Gegenwart	Kagome spin ice HoAgGe
O16	14:30	Rachel Nixon	Expanding investigations into ternary compounds of rare-earth mercurides
O17	15:00	Sudip Malick	Large magnetoresistance and complex magnetism in single-crystalline $EuAg_4Sb_2$
	15:30	***Coffee break***	
	U-compounds (UTe_2)		
O18	16:00	Yoshifumi Tokiwa	Self-reconstruction of order parameter in spin-triplet superconductor UTe_2
O19	16:30	Fabrice Wilhelm	5*f* electron occupancy and hybridization in the UTe_2 superconductor from XANES and XMCD studies.
O20	17:00	Michal Vališka	Ultrasound Study of Field-Induced Superconducting Phases in UTe_2
	17:30 19:00	**Posters + refreshment (List of posters is at the end of program)**	

Thursday 19.06.2025			
	RE-compounds II (Ce)		
O21	09:00	Gertrud Zwicknagl	Unusual orders in $CeRh_2As_2$
O22	09:30	Peter Riseborough	Magnetic Excitations of a Nodally-Hybridized Heavy-Fermion Semi-Metal: Application to CeNiSn
O23	10:00	Jeroen Custers	Magnetic Phase Transitions in Sawtooth-Structured $CeRhSn_2$: Interplay of Frustration and Ordering?
	10:30	***Coffee break***	
	Electronic structure – Theory II		
O24	11:00	Josef Spalek	Quantum statistics near Mott localization: Superexclusion and distinguishability
O25	11:30	Maciej Fidrysiak	Variational framework for quantitative description of quantum collective excitations in correlated systems
	12:00	***Lunch***	
	Transition metals		
O26	14:00	Krishna Pokhrel	Pressure-dependent Magnetism in 2D van der Waals Materials ($CrBr_3$ and VI_3): A Theoretical calculations
O27	14:30	Andrej Kancko	Spin-glass and random-singlet ground-states in $NaCdM_2F_7$ pyrochlore (M = Co^{2+}, Ni^{2+}, Cu^{2+}) and defect-fluorite (M = Mn^{2+}) antiferromagnets
O28	15:00	Petr Čermák	Measurement of Altermagnetic Magnon Splitting in CrSb with Circularly Polarized X-Ray Scattering
	15:30	***Coffee break***	
	Applications		
O29	16:00	Itzhak Halevy	Novel Fission Track Detector for Nuclear Forensics: Integrated Aerogel-Lexan detector to determine the different fission isotope
O30	16:30	Galit Katarivas Levy	Transforming Healthcare through Additive Manufacturing
	17:00	Free time	
	19:00	***Grill party***	
	22:00		
Friday 20.06.2025			
	RE-compounds III (Frustration)		
O31	09:00	Naoto Metoki	Magnetic and quadrupole coupling emerging in NdB_4 with geometrical frustration
O32	09:30	Tim Treu	Utilizing frustration in Gd- and Yb-based oxides for milli-Kelvin adiabatic demagnetization refrigeration
O33	10:00	Sonu Kumar	Magnetoelectric Coupling and Dielectric Anomalies in the Frustrated Quantum Magnet $PrMgAl_{11}O_{19}$
	10:30	***Coffee break***	
	RE-compounds IV		
O34	11:00	Fuminori Honda	Electronic Properties of Eu-Based Compounds under High Pressure
O35	11:30	Dominik Legut	Perpendicular magnetic anisotropy in a single Dy adatom ferrimagnet
	12:00	Summary, Non-structured discussion and excursions to the laboratories	
	14:00		

List of posters

Code	Title	Presenter
P01	Angle-Resolved Photoemission Spectroscopy Study of Kondo Semimetals/Insulators: CeNiSn, CeRhSb, CeRhAs	J.-S. Kang
P02	Magnetic properties of the $Dy_xY_{1-x}(PO_3)_3$ glasses	Vladimír Tkáč
P03	Magnetism of $Nd_{3-x}U_xRu_4Al_{12}$ intermetallic compounds	Alexander Andreev
P04	Pseudogap in slightly doped $Y_{0.77}Pr_{0.23}Ba_2Cu_3O_{7-\delta}$ single crystals	Liudmyla Bludova
P05	High field study of UTe_3	Tetiana Haidamak
P06	Robust pressure effects on magnetic orders in $NiBr_2$	Parvez Ahmed Qureshi
P07	Search for new $REAgBi_2$ compounds	Ivanna Arseniuk
P08	Enhancing Fission Track Analysis for Nuclear Forensics: Image Processing Automation and Aerogel Integration	Itzhak Halevy
P09	Influence of Hafnium on α-UH_3 Phase Stability and Magnetism in Uranium Hydrides	Shanmukh V.V. Uday Devanaboina
P10	Sub-50mK adiabatic demagnetization refrigeration with frustrated Yb- oxide magnets in the PPMS.	Marvin Klinger
P11	Magnetic structure and excitations in the antiferromagnet $Na_2BaMn(PO_4)_2$	David Svitak
P12	LaueDB: A Dataset for Laue Patterns	Štěpán Venclík
P13	Charles Automata: Physics laboratory automation	Tomáš Červeň
P14	EuAl: synthesis, crystal structure and properties	Yurii Prots
P15	Taming Mosaicity with Robotics and AI: The Automatic Laue Sample Aligner (ALSA)	Jan Kříž
P16	Crystal growth of unconventional superconductor UTe_2 and other U-Te intermetallics	Andrej Cabala
P17	Magnetism of $NdMn_{1-x}Ti_xO_3$ system	Marian Mihalik

O01

HERFD vs XAS: The Case for Equivalence

James Tobin

U. Wisconsin-Oshkosh, Oshkosh, USA

The advent of new, powerful, highly efficient, multi-component, X-ray monochromators used in the detection of tender x-rays has revolutionized spectroscopic investigations of the 5f electronic structure. All of the new experiments are, in essence, variants of X-ray Emission Spectroscopy (XES), where the improved monochromatized detection, applied to novel specific decay pathways, plays a key role. In HERFD (High Energy Resolution Fluorescence Detection) a type of Resonant Inelastic X-Ray Scattering (RIXS), the monochromatized XES detection allows the performance of a scattering experiment with vastly improved resolution. It is argued here that HERFD devolves into a higher resolution version of X-Ray Absorption Spectroscopy (XAS). It has been shown that the M_4 and M_5 spectra are essentially direct measurements of the j-specific ($5f_{5/2}$ and $5f_{7/2}$) Unoccupied Density of States (UDOS), which can be directly correlated with the UDOS from Inverse Photoelectron Spectroscopy (IPES) and Bremsstrahlung Isochromat Spectroscopy (BIS). [1-3] Furthermore, a remarkable level of agreement is achieved between a model based upon the UDOS of Th and a series of HERFD and IPES/BIS results with various 5f occupation levels (See Figure 1.) [4-6]. Finally, the historical record of XAS will be examined, demonstrating the success of various resonant decay schemes as measures of the underlying XAS.

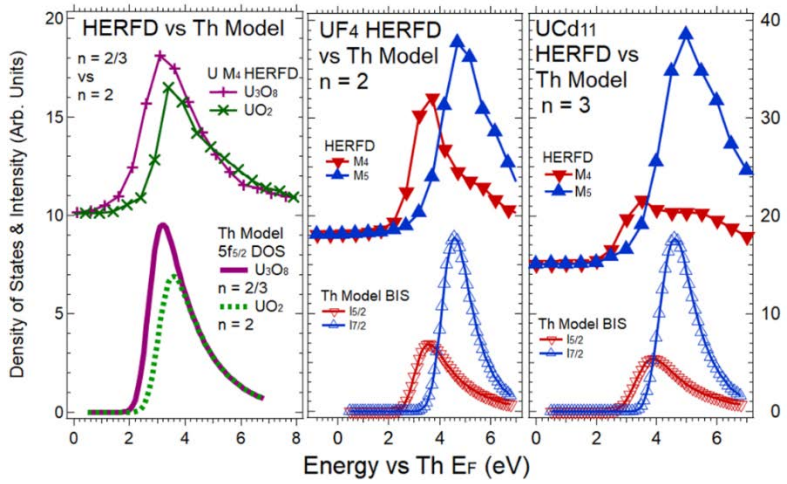

Figure 1. The j-specific Th Model predictions are compared to various HERFD measurements with different 5f occupations (n). [4-6]

[1] J.G. Tobin, H. Ramanantoanina, C. Daul, P. Roussel, S.-W. Yu, D. Sokaras and A. Kutepov, Solid State Sciences 160, 107779 (2025).
[2] J. G. Tobin, H. Ramanantoanina, C. Daul, S.-W. Yu, P. Roussel, S. Nowak, R. Alonso-Mori, T. Kroll, D. Nordlund, T.-C. Weng, D. Sokaras, Phys. Rev. B 105, 125129 (2022).
[3] J. G. Tobin, S. Nowak, C.H. Booth, E.D. Bauer, S.-W. Yu, R. Alonso-Mori, T. Kroll, D. Nordlund, T.-C. Weng, D.Sokaras, J. Elect. Spect. Rel. Phen. 232, 100 (2019).
[4] J. G. Tobin, S. Nowak, S.-W. Yu, P. Roussel, R. Alonso-Mori, T. Kroll, D. Nordlund, T.-C. Weng, D. Sokaras, J. Vac. Sci. Tech. A 39, 043205 (2021).
[5] J. G. Tobin, S. Nowak, S.-W. Yu, P. Roussel, R. Alonso-Mori, T. Kroll, D. Nordlund, T.-C. Weng, D. Sokaras, J. Vac. Sci. Tech. A 39, 066001 (2021).
[6] J. G. Tobin, S. Nowak, S.-W. Yu, P. Roussel, R. Alonso-Mori, T. Kroll, D. Nordlund, T.-C. Weng, D. Sokaras, J. Vac. Sci. Tech. A 40, 033205 (2022).

O02

4f-driven surface effects in lanthanide materials from ARPES and XAS: Reorientation of 4f moments, 2D ferromagnetism, Kondo and Rashba effects

Denis Vyalikh

Donostia International Physics Center (DIPC), Donostia-San Sebastian, Spain
IKERBASQUE, Basque Foundation for Science, Bilbao, Spain

Traditionally, ARPES and XAS have been key tools for investigating the electronic and magnetic properties of lanthanide (Ln)-based materials, with a primary focus on bulk-related phenomena. This is particularly true for numerous XAS measurements performed at the Ln $M_{4,5}$ and $N_{4,5}$ edges, where spectral lineshape analysis is predominantly discussed in the context of bulk effects. In general, the surfaces of Ln materials have received considerably less attention than the bulk. However, it is reasonable to anticipate that 4f-driven physics at the surface could be even richer and compelling than in the bulk. The lack of inversion symmetry, spin-orbit coupling, the emergence of surface states and resonances, relaxation and reconstruction, as well as modifications of the CEF near and at the surface, all serve as driving forces for novel 4f-driven phenomena, distinct phases, and characteristic temperature scales that differ dramatically from those in the bulk.

In this contribution, I will present an overview of the most interesting results recently obtained by our team in studying surface 4f-driven phenomena in lanthanide systems, such as $LnRh_2Si_2$ and $LnIr_2Si_2$, using ARPES and XAS. In particular, I will focus on Ce-based materials, which are well known for their exotic bulk phenomena, including $CeRh_2Si_2$, $CeIrIn_5$, and $CeCo_2P_2$. Additionally, we will consider the valence-fluctuating material $EuIr_2Si_2$, where the divalent behavior of Eu near the surface induces 2D ferromagnetic properties in the Si-Ir-Si-Eu surface block, accompanied by a strong cubic Rashba spin-orbit coupling effect.

Our findings reveal that 4f magnetic moments reorient near the surface due to modifications in the crystal electric field compared to the bulk. By analyzing modeled spectra for each $\mathbf{M_J}$ state in comparison with experimental data, we can conclusively determine the orientation of magnetic moments both in the bulk and at the surface. Furthermore, we provide clear evidence of unexpectedly different Kondo-related properties at the Ce surface and in the bulk, as observed in $CeRh_2Si_2$. The obtained results make a call for detailed studies of the properties emerging at the surfaces of many strongly correlated Ce-, Eu-, and Yb-based materials with quasi-2D structure. They also bear strong implications for how novel functional and quantum materials can be devised using thin layers of *f*-materials as building blocks. In such systems, different combinations of fundamental interactions can be realized.

O03

Can the Valence-to-Core RIXS Measured at the Uranium M_5 Edge Quantify the Uranium–Ligand Hybridization in Insulators like UO_2 and UF_4?

Jindřich Kolorenč

Institute of Physics (FZU) of the Czech Academy of Sciences, Prague, Czech Republic

Motivated by a recent experimental study [1], we model the valence-to-core resonant inelastic x-ray scattering (RIXS) measured at the uranium M_5 edge in insulating compounds UO_2 and UF_4. We employ the Kramers–Heisenberg formula in conjunction with the Anderson impurity model extracted from the corresponding LDA+DMFT electronic-structure calculations [2], in which the double-counting correction is adjusted to best reproduce the experimental valence-band XPS spectra [3,4]. We find two sets of excited states: One group is formed by excitations of the $5f^2$ shell that appear at energy losses $\lesssim 4$ eV. These excitations are not well resolved in the experimental data [1] as they are largely obscured by the elastic peak (except in the new high-resolution data report very recently [5]). The other group of excited states is comprised of charge-transfer excitations corresponding to a transfer of an electron from the oxygen/fluor 2p states to the uranium 5f shell. We identify these excitations with the spectral feature experimentally observed at an energy loss of roughly 8–10 eV, in agreement with other investigations [6,7]. Our model estimates the intensity, with which the charge-transfer excitations appear in the RIXS spectra, to be larger in UO_2 than in UF_4, just like it is observed in the experiment [1]. We analyze in some detail how this intensity depends on the strength of the metal-ligand hybridization and on other quantities, such as the magnitude of the core-valence interaction acting in the intermediate state of the RIXS process. Finally, we discuss how the RIXS spectra would look in simple band insulators as opposed to Mott insulators like UO_2 and UF_4.

[1] J. G. Tobin et al., J. Phys.: Condens. Matter 34, 505601 (2022).
[2] J. Kolorenč, A. Shick, A. Lichtenstein, Phys. Rev. B 92, 085125 (2015).
[3] Y. Baer, J. Schoenes, Solid State Comm. 33, 885 (1980).
[4] A. Yu Teterin et al., Phys. Rev. B 74, 045101 (2006).
[5] A. Severing et al., 54èmes Journées des Actinides (2025).
[6] K. Kvashnina et al., Chem. Commun. 54, 9757 (2018).
[7] K. Kvashnina et al., Phys. Rev. B 95, 245103 (2017).

O04

XAS studies of U hydrides and other U systems - a key to the 5*f* occupancy?

Ladislav Havela

Charles University, Prague, Czech Republic

In transition-metal compounds, energies of $L_{2,3}$ X-ray absorption edges have been traditionally used to identify multiple valence (oxidation) states. The *L* absorption spectrum is dominated by dipole transitions from the core 2*p* level to the open *d* shell of a transition metal. The dipole transition energies and the transition probabilities depend on the local electronic structure. An important precondition is that the 2*p* core-hole lifetime broadening allows to distinguish individual valence states, separated by several eV. This naturally applies to non-metallic compounds with distinct localized *d* states.

The same technique turned useful in identifying valence fluctuation in anomalous rare-earths. Multiple absorption edges corresponding to distinct oxidation states could mean that there may be more RE positions, each with a different 4*f* occupancy, changing dramatically the 2*p*-4*f* Coulomb repulsion. But if this happens for a compound with one RE site, it implies valence fluctuations (mixed valence, intermediate valence), with the fast XAS process catching, with varying probability, always one of the two terminal valence states.

The most interesting case of actinides provides both the $L_{2,3}$ edges reflecting the 2*p* to 6*d* excitations and the $M_{4,5}$ edges reflecting the 3*d* to 5*f* excitations. However, to distinguish individual valencies is rather challenging for conventional XAS due to smaller energy separation compared to the lifetime broadening. A breakthrough came with the HERFD (High Energy Resolution Fluorescence Detection) mode, selecting only one deexcitation channel (e.g. 4*f* to 3*d*), which is particularly slow due to the 4*f* core-hole lifetime. This brought a reliable scale of absorption energies as a function of oxidation state in non-metallic compounds, e.g. identifying U^{3+}, U^{4+}, U^{5+}, U^{6+} states in various compounds. Such situation raised expectations in determination if there are 2 or 3 5*f* electrons in URu_2Si_2 and other exotic systems, at which the 5*f* occupancy is a game changer in terms of a particular microscopic model used. The discussion of several cases including U metal will show why this technique does not generally provide an ultimate solution of the $5f^n$ issue. The reason is a variable 5*f* delocalization, modulating the Coulomb repulsion between 5*f* and core-level states. However, there are situations in which it can still give a very strong hint.

This work was supported by the Czech Science Foundation under the grant # 25-16339S.

O05

Revisiting arsenides – from simple to complex

Eteri Svanidze

MPI CPfS, Dresden, Germany

Based on the chemical similarities between f-elements and alkali/alkali earths, we can stipulate the formation of f-electron-based compounds with the architecture of iron-arsenides [1]. And while these compounds are not likely to be high-Tc superconductors, we can use their small energy scales for an easy tuning from one ground state to another.

Surprisingly, only a handful of stoichiometries has been discovered among the lanthanide/actinide-iron-arsenic compounds [2, 3] which is perhaps a result of synthesis complications imposed by toxicity and high vapor pressure of constituent elements. In this talk, I will discuss new compounds that we have discovered within the U-Fe-As [4, 5], Sm-Fe-As [6,7], Yb-Fe-As [8] and Pr-Fe-As [8] ternaries. All of the new arsenides were synthesized in single crystalline form. I will discuss the interesting properties these new compounds show – negative thermal expansion, room temperature giant magnetoresistance, magnetic order above room temperature, complex magnetic configurations, as well as enhanced effective electron mass. I will then describe how these properties can be understood by relating the crystal structure of these novel materials to well-known arsenides.

E.S. is grateful for the support of the Christiane Nusslein-Volhard-Stiftung E.S., N. Z. and M. K. acknowledge the support of the Boehringer Ingelheim Plus 3 Program. N.Z. is grateful for the support of the Humboldt Foundation through the Philipp Schwartz Initiative.

[1] Q. Si and N. E. Hussey, Physics Today 76, 34 (2023).
[2] D. Kaczorowski, Journal of Alloys and Compounds 186, 333 (1992).
[3] W. Jeitschko, R. Brink, P.G. Pollmeier, Zeitschrift für Naturforschung 48, 52 (1993).
[4] N. Zaremba, M. Krnel, Yu. Prots, A. Leithe-Jasper, Yu. Grin, L. Akselrud, E. Svanidze, Inorganic Chemistry 63, 5414 (2024).
[5] N. Zaremba, M. Krnel, Yu. Prots, A. Leithe-Jasper, Yu. Grin, L. Akselrud, E. Svanidze, in preparation (2025)
[6] O. Karychort, N. Zaremba, M. Krnel, Yu. Prots, A. Leithe-Jasper, Yu. Grin, L. Akselrud, E. Svanidze, in preparation (2025).
[7] I. Robredo, Y. Fang, L. Chen, N. Zaremba, Y. Prots, M. Krnel, M. Koenig, T. Doert, J. van der Brink, C. Felser, Q. Si, E. Svanidze, M. G. Vergniory, arXiv: 2505.01511 (2025).
[8] O. Karychort, N. Zaremba, M. Krnel, Yu. Prots, A. Leithe-Jasper, L. Akselrud, Yu. Grin, E. Svanidze, in preparation (2025).

O06

A new family of topological insulators RAsS (R = Y, La, Sm)

Mitja Krnel, Nazar Zaremba, Yurii Prots, Eteri Svanidze

Max Planck Institute for Chemical Physics of Solids, Dresden, Germany

Numerous *d*-electron compounds and lanthanides have been identified as topological insulators (TI) [1]. In topological insulators the conductive surface states exist in parallel with the insulating bulk and are protected by symmetry. We report the discovery of three new TIs, YAsS, LaAsS, and SmAsS, where the SmAsS is a heavy-fermion compound and LaAsS is close to a topological transition [2]. We show that the symmetry of the structure preserves the surface states. The previously reported monoclinic structure of the compounds (space group $P112_1/n$) was reexamined and resolved as orthorhombic (space group *Pnma*) by using high-resolution XRD with synchrotron radiation. YAsS, LaAsS, and SmAsS show different types of deformation (YAsS and SmAsS have orthorhombic distortion along tetragonal axes *a* and *b*, whereas LaAsS has deformation along the diagonals. We demonstrate that YasS and SmAsS structures can host glide-symmetry-protected Hourglass fermions, which are topological surface states with dispersion relation shaped like an hourglass [3]. By using DFT we calculate the band structure and construct the irreducible representations at high symmetry points of the structure [4]. In order to characterize the topological properties of the system, we calculate the symmetry indicator (topological invariant) for all three compounds [2, 5]. It turns out that the topological invariant is not dependent on the presence of spin-orbit coupling, which classifies the topological insulators as topological crystalline insulators. The measured specific heat of SmAsS confirms that it is a heavy-fermion compound with $\gamma = 160$ mJ mol_{Sm}^{-1}. In SmAsS the surface states survive despite *f*-electron interactions present in the compound, they just shift in energy, which classifies SmAsS as a strongly correlated topological crystalline insulator.

O07

New uranium-cobalt-arsenides with antiferromagnetic ordering

Nazar Zaremba[1], Mitja Krnel[1], Yurii Prots[1], Lev Akselrud[2], Markus König[1], Yurii Grin[1], Eteri Svanidze[1]

[1]Max-Planck-Institut für Chemische Physik fester Stoffe, Dresden, Germany
[2]Ivan Franko National University of Lviv, Lviv, Ukraine

Uranium-based materials remain significantly less explored, compared to their rare-earth analogues, mostly as a result of their fragile ground states coupled with non-trivial synthetic requirements. Among binary compounds in the U−Co and U−As phase space, both superconductivity and magnetism are found. Interestingly, the most uranium-rich uranium-cobalt binary U_6Co compound displays phonon-mediated superconductivity below T_c = 2.4 K [1]. The UCo_2 [2,3] and UCo_3 [4] compounds are both paramagnets. While the most cobalt-rich compound $UCo_{5.3}$ orders ferromagnetically above room temperature (T_C = 360 K [5,6]). In the U-As binary, UAs [7] and UAs_2 [8] show antiferromagnetic transitions at 126 and 283 K, respectively, while U_3As_4 is a ferromagnet below T_C = 198 K [9]. Within the Co-As binary, both $CoAs_2$ [10] and $CoAs_3$ [11] are diamagnets, Co_2As [12] is ferrimagnetic below 60 K, while CoAs is a paramagnetic material. A natural extension into the U-Co-As was successful in discovering two compounds – $U_2Co_{12}As_7$ [13] and $UCoAs_2$ (T_C = 144 K) [14]. By implementing flux synthesis, we could grow large single crystals of $U_8Co_{42}As_{25}$ ($Y_8Co_{41}As_{25}$ str. type [15], *P*6$_3$/*m*, *hP*82, a = 17.7460(5) Å, c = 3.8120(1) Å) and UCo_3As_2 ($HoCo_3P_2$ [16] str. type, *Pmmn*, *oP*38, a = 3.8623(2) Å, b = 10.8416(6), c = 12.7265(7) Å). Both compounds order antiferromagnetically below T_N = 25 and 65 K, respectively.

[1] B. S. Chandrasekhar et al., J. Phys. Chem. Solids. 7, 259-267 (1958).
[2] M. Zeleny, et. al., Phys. Stat. Sol. (a) 57: K17-K20 (1980).
[3] E. Burzo, et. al., Solid State Communications 56, 537-539 (1985).
[4] I. Lupsa, P. Lucaci, and E. Burzo, J. Alloys Comp. 204, 247-250 (1994).
[5] A. V. Deryagin et al., Zh. Eksp. Teor. Fiz. 44, 610 (1976).
[6] A. Dommann, et al., J. Less-Common Metal 158, 287 (1990).
[7] G. H. Lander et al., Phys. Rev. B 10, 1994 (1974).
[8] W. Trzebiatowski, et al., Bull. Acad. Polon. Sci., Ser. Sci. Chem. 12 (1964).
[9] C. F. Sampson, et al., Journal of Physics C: Solid State Physics 9, 4035 (1976).
[10] A. Kjekshus, et al., Acta Chem. Scand. 25, 411 (1971).
[11] D. J. Campbell, et al., Physical Review B 97, 174410 (2018).
[12] A. Kjekshus, et. al., Svensson, Acta Chem. Scand. 26, 2554 (1972).
[13] W. Jeitschko, et al., Dalton Trans. 39, 6067 (2010).
[14] D. Kaczorowski, J. Alloys Comp. 186, 333 (1992).
[15] V. Babizhetskyy et. al., Visnyk of the Lviv University. Series Chemistry 64, 110 (2023).
[16] W. Jeitschko et. al., J. Less-Common Metals 110, 339 (1985).

O08

Magnetic Susceptibility of $YbRh_2Si_2$

Petra Knappová[1,2], Marijn Lucas[1], Jan Knapp[1], Lev Levitin[1], Brian Cowan[1], Andrew Casey[1], John Saunders[1]

[1]Royal Holloway University of London, Egham, United Kingdom
[2]TU Dresden, Dresden, Germany

The heavy-fermion metal $YbRh_2Si_2$ becomes superconducting below approximately 10 mK and is a candidate for odd-parity, and hence topological, superconductivity. Recent studies have established a detailed magnetic phase diagram, revealing the emergence of a novel phase characterized by electro-nuclear spin density wave order below 1.5 mK [1,2]. $YbRh_2Si_2$ exhibits a remarkable interplay between superconductivity and antiferromagnetism, as demonstrated by electrical transport and heat capacity measurements. In particular, superconductivity initially develops heterogeneously, but below 1.5 mK it is significantly enhanced, stabilizing the topological helical phase [3]. Here we report measurements of the low-frequency complex AC susceptibility and DC magnetization performed with the sample externally shielded to magnetic fields below 20 nT, and with field applied perpendicular to the crystallographic c-axis. The map of the AC susceptibility in the H-T plane is consistent with that inferred from electrical transport, and confirms the boost in superconductivity at 1.5 mK. The DC magnetization results allow us to set an upper bound on the lower critical field, which is particularly small because the system has low T_c and is an extreme type-II superconductor. In the region of heterogeneous superconductivity, above 1.5 mK, we analyze the AC susceptibility in terms of an effective London penetration depth λ. This has an unusual temperature dependence with a significantly larger effective $\lambda(0)$ than anticipated, which also displays a strong effective non-linear Meissner effect.

[1] J. Knapp et al., Electronuclear transition into a spatially modulated magnetic state in $YbRh_2Si_2$. Phys. Rev. Lett., 130, 126802 (2023).
[2] J. Knapp et al., Magnetic phase diagram of $YbRh_2Si_2$: the influence of hyperfine interactions, arxiv.org/abs/2501.17560 (2025).
[3] L. Levitin et al., Odd-parity superconductivity underpinned by antiferromagnetism in heavy fermion metal $YbRh_2Si_2$, arxiv.org/abs/2502.06420, (2024).

O09

The Heavy Fermion $YbRh_2Si_2$ – Spin Triplet Superconductor Underpinned by Antiferromagnetism

Jan Knapp[1,2], Lev Levitin[1], Jan Nyéki[1], Andrew Ho[1], Brian Cowan[1], Manuel Brando[2], Christoph Geibel[2], Kristine Kliemt[3], Cornelius Krellner[3], John Saunders[1]

[1]Royal Holloway University of London, Egham, United Kingdom
[2]Max Planck Institute for Chemical Physics of Solids, Dresden, Germany
[3]Goethe University, Frankfurt, Germany

The heavy fermion metal $YbRh_2Si_2$ has been extensively studied for many years as an example of a system that can be tuned towards quantum criticality, by chemical pressure or by magnetic field. Our calorimetry and electrical transport measurements down to temperatures below 1 mK allowed us to determine the magnetic phase diagram of natural $YbRh_2Si_2$ [1,2,3], featuring two antiferromagnetic phases, electronic AFM1 and electro-nuclear AFM2, both terminating at field-tuned quantum phase transitions. Stability of the large moment electro-nuclear spin density wave phase we refer to as AFM2 and the backturn of the critical field of AFM1 are both manifestations of the hyperfine interaction of Yb. The hyperfine constant is particularly strong, $A_{hf} = 102\ \mu_B/T$, and combined with the strong dependence of 4f Yb moment on in-plane field leads to dramatic effects, despite only 30% of Yb nuclear moments carrying a magnetic moment in natural $YbRh_2Si_2$.

Superconductivity onsets in $YbRh_2Si_2$ below 10 mK, making the material only the second Yb-based heavy fermion discovered. Our high-resolution measurements of the complex electrical impedance reveal the presence of two distinct superconducting states, suppressed differently by magnetic field, both Pauli-limited and beyond the Pauli limit [3]. Superconductivity is abruptly switched off at the critical field of AFM1 and dramatically enhanced by the transition into AFM2 (T_A). We understand this boost by the simultaneous formation of a spin-triplet pair density wave. Together these observations provide compelling evidence for odd-parity superconductivity, and its underpinning by antiferromagnetism, and allow us to identify the topological helical state.

[1] J. Knapp et al., Electronuclear transition into a spatially modulated magnetic state in $YbRh_2Si_2$. Phys. Rev. Lett., 130, 126802 (2023).
[2] J. Knapp et al., Magnetic phase diagram of $YbRh_2Si_2$: the influence of hyperfine interactions, arxiv.org/abs/2501.17560 (2025).
[3] L. Levitin et al., Odd-parity superconductivity underpinned by antiferromagnetism in heavy fermion metal $YbRh_2Si_2$, arxiv.org/abs/2502.06420, (2024).

O10

NEW HEAVY FERMION COMPOUND $Ce_6Rh_{30}As_{19}$: CRYSTAL STRUCTURE AND PHYSICAL PROPERTIES

Oksana Karychort[1,2], Mitja Krnel[2], Yurii Prots[2], Nazar Zaremba[2], Yuri Grin[2], Olga Zhak[1], Eteri Svanidze[2]

[1]Ivan Franko National University of Lviv, Lviv, Ukraine
[2]Max Planck Institute for Chemical Physics of Solids, Dresden, Germany

The strong influence of cerium's 4*f*-electrons on magnetic interactions in compounds containing Ce and *d*-elements such as Rh has been a subject of considerable interest in condensed matter physics. These arsenides are particularly fascinating due to their potential electronic and superconducting properties. Among the ternary arsenides of cerium and rhodium, CeRhAs has been observed to exhibit a Kondo-insulator pseudo-gap, with an estimated gap size of 0.5 ± 0.1 eV [1,2]. In contrast, $CeRh_2As_2$ has attracted significant attention due to its unconventional superconducting properties, undergoing two superconducting transitions with T_{C1} = 0.4 K and T_{C2} = 0.26 K [3,4].

Despite the intriguing properties revealed by CeRhAs and $CeRh_2As_2$, no additional compounds containing cerium, rhodium, and arsenic had been identified so far. In this work, we revisit the Ce–Rh–As system and report the discovery of a new compound, $Ce_6Rh_{30}As_{19}$, synthesized using the metal flux technique. The new arsenide crystallizes in the hexagonal space group $P6_3/m$ and adopts the $Sm_6Rh_{30}As_{19}$-type structure, with lattice parameters a = 16.0887(5) Å and c = 3.9318(2) Å.

Magnetic properties measurements of $Ce_6Rh_{30}As_{19}$ reveal antiferromagnetic ordering below 2 K. Specific heat data indicate heavy-fermion behavior, as evidenced by a large Sommerfeld coefficient of γ = 900 $mJ \times mol^{-1} \times K^2$.

[1] T. Ekino, et al., Physica B Condens. Matter., 312–313, 221–223 (2002).
[2] F. Ishii and T. Oguchi, J. Physical Soc. Japan, 73(1), 145–151 (2004).
[3] S. Khim et al., Phys. Rev. B 111(11), 115134 (2025).
[4] J. F. Landaeta et al., Phys. Rev. X, 12, (3), 031001 (2022).

O11

Hybrid Superconducting Devices

Anamaria Ghihor, Yejin Lee, Haolin Jin, Andreas Leithe-Jasper, Markus Konig, Mitja Krnel, Eteri Svanidze, Uri Vool

Max Planck Institute for Chemical Physics of Solids, Dresden, Germany

Superconducting resonators are highly tunable, low-loss coherent macroscopic devices, making them ideal for quantum technology and sensing applications. Recently, these resonators have been paired with van der Waals (vdW) materials to explore their microwave losses, dielectric properties and kinetic inductance.[1] However, creating a hybrid device that only integrates a superconducting resonator with a vdW flake limits the range of materials that can be used. In order to overcome this challenge, we can fabricate a 'lamella' that replicates the flake using the focus ion beam (FIB). Another advantage of this technique is that it enables precise control over the dimensions of the lamella, something that is not possible when working with flakes. This lamella can then be attached in-situ on the resonator using a micromanipulator.[2] This powerful technique allows the exploration of a wide range of materials and their behavior. UBe_{13}, was chosen due to its unusual superconductivity and properties. Typically, unconventional superconductivity arises near a suppressed magnetic phase, as seen in compounds like, electron-doped cuprates, organic superconductors, and heavy fermion materials.[3] In these cases, the Cooper pairing mechanism is thought to be influenced by fluctuations in the magnetic order parameter. However, UBe_{13}, a heavy fermion superconductor, stands apart from this pattern, as no magnetic phase has been identified, leaving the origin of its unconventional superconductivity unresolved.[4] The project focuses on fabricating devices like resonators using FIB to investigate the behavior of this material and how the microwave response of the hybrid circuit changes when this material is incorporated.

[1] H. Jin, G. Serpico, Y. Lee, and U. Vool, "Exploring van der Waals Cuprate Superconductors Using a Hybrid Microwave Circuit ", Nano Letters 25 (8), 3191-3198 (2025).
[2] A. Antonyshyn, M. Bobnar, O. Sichevych, and Yu. Grin, "Micro-scale device - an alternative route for studying the intrinsic properties of solid-state materials: the case of semiconducting TaGeIr", Angewandte Chemie International Edition 59, 11136 (2020).
[3] A. Amon, E. Svanidze, A. Ormeci, and Yu. Grin, "Interplay of atomic interactions in the intermetallic semiconductor Be_5Pt", Angewandte Chemie International Edition 58, 15928 (2019).
[4] A. Amon, I. Zelenina, P. Simon, and Yu. Grin, "Tracking aluminum impurities in single crystals of the heavy-fermion superconductor UBe_{13}", Scientific Reports 8, 10654 (2018).

O12

Synthesis and superconductivity of Be-based compounds

Özlem Evren[1], Ali Arda Aydın[2], Nazar Zaremba[1], Mitja Krnel[1], Andreas Leithe-Jasper[1], Yuri Prots[1], Yuri Grin[1], Eteri Svanidze[1]

[1]Max Planck Institute for Chemical Physics of Solids, Dresden, Germany
[2]Koç University, College of Sciences, Istanbul, Turkey

Structural chirality can sometimes lead to interesting effects like non-centrosymmetric magnetism, Weyl fermions, and skyrmions. BeAu is an unconventional superconductor with a noncentrosymmetric B20 crystal structure [1–5]. Its intriguing properties, combined with a relatively simple structure that facilitates computational modeling, have attracted considerable interest from theorists [4,5]. Recent studies have expanded to other Be–Au compositions as well, revealing a rich landscape of potential phases [6,7]. However, experimental understanding of its properties remains limited, primarily due to the lack of available single crystals [5]. Overcoming this barrier would not only enable detailed studies of BeAu itself but also provide broader insights into the field of unconventional superconductivity.
In this work, we explore various synthesis approaches in order to obtain single crystals of BeAu. In addition to targeting the 1:1 stoichiometry, we also aim to synthesize other Be-Au phases, which have been predicted to exist theoretically. We further explore the ternary compositions containing Be and Au, with focus on systems that have not been examined yet.

[1] A. Amon et al., Physical Review B. 97 (2018), doi:10.1103/physrevb.97.014501.
[2] R. Khasanov, R. Gupta, D. Das, A. Leithe-Jasper, E. Svanidze, Physical Review B. 102 (2020), doi:10.1103/physrevb.102.014514.
[3] R. Khasanov et al., Physical Review Research. 2 (2020), doi:10.1103/physrevresearch.2.023142.
[4] A. Bhowmick, J. Singh, V. Kanchana, Physical Review B. 111 (2025), doi:10.1103/physrevb.111.115122.
[5] R. Khasanov et al., Physical Review B. 111 (2025), doi:10.1103/physrevb.111.104507.
[6] B. Jin, Z.-R. Wang, Y.-J. Wang, Dalton Transactions (2025), doi:10.1039/d5dt00170f.
[7] M.-H. Wang et al., Chemical Science. 13, 11099–11109 (2022).

O13

Acoustic signatures of the field-induced electronic-topological transitions in $YbNi_4P_2$

Jeremy Sourd[1], E.-O. Eljaouhari[2,3], K. Kliemt[4], C. Krellner[4], J. Wosnitza[1,5], S. Zherlitsyn[1], G. Zwicknagl[6,7]

[1]High Magnetic Field Laboratory (HLD-EMFL), HZDR, Dresden, Germany
[2]Institut für Mathematische Physik, Braunschweig, Germany
[3]Laboratoire Ondes et Matière d'Aquitaine, Bordeaux, France
[4]Physikalisches Institut, Johann Wolfgang Goethe-Universität, Frankfurt, Germany
[5]Institute of Solid State and Materials Physics, Dresden, Germany
[6]Institut für Mathematische Physik, Braunschweig, Germany
[7]Max Planck Institute for Chemical Physics of Solids, Dresden, Germany

The Fermi surface is a central concept to elaborate the physical properties of correlated electron systems. While resulting from the precise chemistry of a given material through its crystal and electronic structures, the Fermi surface shape and topology can evolve drastically upon varying a control parameter leading to an electronic topological transition (ETT).

In heavy-fermion compounds the strong electronic correlations may generate renormalized flat bands close to the Fermi level, leading to effective Fermi energies of the order of 10 T. Thus, in these systems the Zeeman energy from moderate magnetic field is enough to induce an ETT. A particularly interesting example of this physics is the ferromagnetic heavy-fermion compound $YbNi_4P_2$, which shows a very complex electronic structure with multiple field-induced ETTs below 18 T [1].

We used acoustic waves of different symmetry in order to probe the sequence of ETT in $YbNi_4P_2$, by performing ultrasound measurements at low temperatures. We report a series of anomalies in the sound velocity, as well as magnetoacoustic quantum oscillations in agreement with the sequence of ETTs reported in [1]. Furthermore, our results show that different acoustic modes are more sensitive to different ETTs. In order to discuss this aspect, we developed a microscopic model adapted to the strongly correlated electronic structure of $YbNi_4P_2$, which allows to derive realistic couplings between the electronic states and the sound waves. This shows how ultrasound permits to explore the ETTs in $YbNi_4P_2$, by analyzing electron-phonon couplings in reciprocal space for each acoustic mode.

[1] Pfau et al., Phys. Rev. Lett. 119(12), 126402 (2017).

O14

Strongly electron-correlated atomic-like approach to 3*d*/4*f*/5*f*/4*d*/5*d*/ compounds

Ryszard Radwanski, Zofia Ropka

Center of Solid State Physics, Krakow, Poland

There is a rapidly growing number of experiments confirming the author's 35-years scientific project "From the atomic physics to solid-state physics: UPd_2Al_3" which one could call as Quantum Atomistic Solid-State Theory (QUASST). QUASST starts theoretical description of a solid containing open d/f shell atoms from analysis of the atomic-scale charge distribution, the realized atomic valency and the atomic-like term of the involved 3*d*/4*f*/5*f*/4*d*/5*d* ions. Being specific we mention $FeBr_2$ [1] and $LaCoO_3$ [2], having Fe^{2+} and Co^{3+} ions. Despite different valences both these ions are strongly-electron correlated system $3d^6$. $FeBr_2$ and $LaCoO_3$ are nice exempla of high and low-spin configurations $t_{2g}^4e_g^2$ and t_{2g}^6, respectively, with octahedral subterms $^5T_{2g}$ (^{5}D term) and $^1A_{1g}$ (^{1}I term). Realization of different octahedral subterms is directly the effect of the strength of crystal-field interactions according to Tanabe-Sugano diagrams. Low-energy electronic structure, below 25 meV, is determined by crystal-field and spin-orbit interactions. Crystal field effect is a multipolar Stark effect known in the atomic physics. Similarly, in the magnetically-ordered state one deals with the Zeeman effect.

We claim that i) the conventional crystal-field interactions should be evaluated the first for any meaningful description of magnetic and electronic properties of any 3*d*/4*d*/5*d*/4*f*/5*f* compound, ii) in such compounds there exists the discrete electronic structure, giving effects close to the Fermi surface at the energy scale even below 1 meV, iii) the 3*d*/4*f*/5*f*/4*d*/5*d* electrons exhibit a substantial localized character maintaining strongly-correlated $3d^n/4d^n/5d^n$ configurations, and iv) the standard band structure calculations, in the eV-energy scale, should be complemented with this discrete low-energy atomic-scale electronic structure.

In recently studied systems like $NbSe_2$ or $MoSe_2$ and Ba_2NaOsO_6 or Ba_2CaOsO_6 (and many many others) the 4*d*/5*d* ions are regarded as Nb^{4+} ($4d^1$), Mo^{4+} ($4d^2$), Os^{7+} ($5d^1$) and Os^{6+}($5d^2$) confirming that the localized QUASST theoretical approach, based on the old crystal field theory of Van Vleck, Bethe, Goodenough is widely used ruling out the band theories with d-shell bands wide for more than 1 eV.

[1] Z. Ropka, R. Michalski, R. J. Radwanski, Phys. Rev. B 63, 172404 (2001).
[2] Z. Ropka, R. J. Radwanski, Phys. Rev. B 67, 172401 (2003).

O15

Kagome spin ice HoAgGe

Philipp Gegenwart

University of Augsburg, Augsburg, Germany

Spin ice denotes a novel state of matter, arising in certain geometrically frustrated magnets that do not have a single minimal-energy state but rather fulfill an ice constraint, leading to highly degenerate local spin configurations. While three-dimensional pyrochlore spin ice is well established, its two-dimensional counterpart “Kagome spin ice”, with 2 in-1 out or 1 in-2-out ice rule, leading to a honeycomb lattice of positive/negative magnetic monopoles, was only studied on artificial nanorods of ferromagnet films. The rare-earth intermetallic HoAgGe has non-Kramers $4f^{10}$ moments on a distorted kagome lattice with the four lowest CEF modes contributing to magnetism at low temperatures. Remarkably the in-plane magnetization at low temperatures reveals a series of metamagnetic transitions separating fractional magnetization plateaus. Refinement of single crystal neutron diffraction reveals that all these states fulfill the kagome ice rule, establishing HoAgGe as first crystalline kagome spin ice [1]. Magnetotransport and anomalous Hall effect (AHE) show pronounced signatures related to the transitions between the fractional magnetization plateaus. They allow to distinguish domains with opposite toroidal orders and differing AHE yet similar magnetization, implying a hidden time-reversal-like degeneracy, related to the non-trivial distortion of the kagome lattice in HoAgGe [2]. Furthermore, we elucidate the nature of ground state of the with broken time-reversal symmetry. Work in collaboration with Kan Zhao and Hua Chen.

[1] K. Zhao, H. Deng, H. Chen, K.A. Ross, V. Petricek, G. Günther, M. Russina, V. Hutanu, P. Gegenwart: Realization of the kagome spin ice state in a frustrated intermetallic compound, Science 367, 1218 (2020).
[2] K. Zhao, Y. Tokiwa, H. Chen, P. Gegenwart: Time-reversal-like degeneracies distinguished by the anomalous Hall effect in a metallic kagome ice compound, Nat. Phys. 20, 442 (2024).

O16

Expanding investigations into ternary compounds of rare-earth mercurides

Rachel Nixon[1,2], Mitja Krnel[1], Nazar Zaremba[1], Marcus Schmidt[1], Lev Akselrud[1,3], Yuri Grin[1], Eteri Svanidze[1]

[1]Max Planck Institute for Chemical Physics of Solids, Dresden, Germany
[2]University of St Andrews, St Andrews, United Kingdom
[3]Ivan Franko Lviv National University, Lviv, Ukraine

Mercury has been an element of intrigue for centuries [1], and continues to play pivotal roles in solid-state chemistry and condensed matter physics [2-6]. However, due to experimental challenges of mercury-based systems – high vapour pressure, toxicity, and extreme air-sensitivity – these compounds are frequently understudied and remain largely unexplored in the scientific literature. In this talk I will outline how we address these technical challenges, with the development of specialised techniques, to study the chemical and physical properties of these anomalous compounds [7-11]. In particular, I will focus on mercury-based ternary systems – motivated by the complex and curious behaviour observed in other mercury-containing materials [8-11]. Ternary mercurides containing both rare-earth and transition-metal elements are exceptionally rare, with only 16 compounds currently reported in databases [12-14]. I will present our motivations and previous results on these distinctive materials [15], together with our ongoing exploratory work on new ternary systems. Through this work we aim to gain deeper insight into the complex chemistry and physics governing these fascinating compounds.

[1] M. Marchini et al., Proc. Natl. Acad. Sci. U. S. A. 119, e2123171119 (2022).
[2] H. K. Onnes, Commun. Phys. Lab. Univ. Leiden, 1911, 120b (1911).
[3] M. König et al., Science 318, 766–770 (2007).
[4] H. Schwer et al., Physica C 243, 10–18 (1995).
[5] J. Karpinski, Philos. Mag. 92, 2662–2685 (2012).
[6] H. Mukuda et al., Phys. Rev. Lett. 96, 087001 (2006).
[7] A. Leithe-Jasper, H. Borrmann and W. Hönle, Max Planck Institute for Chemical Physics of Solids, Scientific Report, Max-Planck-Gesellschaft, Dresden (2006).
[8] K. Witthaut et al., ACS Org. Inorg. Au 3, 143–150 (2023).
[9] Y. Prots et al., Inorg. Chem. 61, 15444–15451 (2022).
[10] Y. Prots et al., Phys. Rev. B 106, L060412 (2022).
[11] E. Svanidze et al., Phys. Rev. B 99, 220403 (2019).
[12] N. P. Gavaleshko et al., Izv. Akad. Nauk SSSR, Neorg. Mater. 21, 1965–1966 (1985).
[13] F. Merlo, M. Pani and M. L. Fornasini, J. Alloys Compd. 196, 145–148 (1993).
[14] A. Iandelli, J. Alloys Compd. 203, 137–138 (1994).
[15] R. Nixon et al., Front. Mater. 11, 3389 (2024).

Acknowledgements: Authors are grateful for the funding provided by the German Research Foundation (DFG-528628333 “Complex compounds based on mercury“).

O17

Large magnetoresistance and complex magnetism in single-crystalline $EuAg_4Sb_2$

Sudip Malick[1,2], Hanna Świątek[1,2], Joanna Bławat[3], John Singleton[3], Tomasz Klimczuk[1,2]

[1]Faculty of Applied Physics and Mathematics, Gdansk University of Technology, Narutowicza 11/12, 80-233, Gdansk, Poland
[2]Advanced Materials Center, Gdansk University of Technology, Narutowicza 11/12, 80-233, Gdansk, Poland
[3]National High Magnetic Field Laboratory, Los Alamos National Laboratory, NM 87545, Los Alamos, USA

The discovery of chiral magnetic anomalies, the anomalous Hall effect, and the topological Hall effect in magnetic topological materials has drawn significant attention to Eu-based compounds as they offer an ideal platform for studying the interplay between magnetism and band topology. Here, we present a thorough investigation of the physical properties of a potential topological material, $EuAg_4Sb_2$, using magnetization, heat capacity, and electrical resistivity measurements. High-quality single crystals were grown using the flux method. Temperature-dependent magnetization measurements along different crystallographic orientations confirm two antiferromagnetic phase transitions around T_{N1} = 10.5 K and T_{N2} = 7.5 K. Isothermal magnetization data exhibit several metamagnetic transitions below T_{N1}. Antiferromagnetic phase transitions in $EuAg_4Sb_2$ are further confirmed by two sharp peaks in the temperature-dependent heat capacity and resistivity data, which shift to lower temperatures in the presence of an external magnetic field. Our systematic heat capacity measurements utilizing a long-pulse and single-slope analysis technique allow us to detect a first-order phase transition in $EuAg_4Sb_2$ at 7.5 K. The magnetoresistance exhibits a broad hump due to the field-induced metamagnetic transition. Remarkably, the magnetoresistance keeps increasing without showing any tendency to saturate as the applied magnetic field increases, and it reaches ~20000% at 1.6 K and 60 T. At high magnetic fields, several magnetic quantum oscillations are observed, indicating a complex Fermi surface. The *H-T* phase diagram constructed using magnetization, heat capacity, and magnetotransport data indicates complex magnetic behavior in $EuAg_4Sb_2$.

O18

Self-reconstruction of order parameter in spin-triplet superconductor UTe_2

Yoshifumi Tokiwa[1], Petr Opletal[1], Hironori Sakai[1], Katsunori Kubo[1], Shinsaku Kambe[1], Etsuji Yamamoto[1], Motoi Kimata[1], Satoshi Awaji[2], Takahiko Sasaki[2], Dai Aoki[3], Yoichi Yanase[4], Yo Tokunaga[1], Yoshinori Haga[1]

[1]Japan Atomic Energy Agency, Tokai, Japan
[2]Tohoku University, Sendai, Japan
[3]Tohoku University, Oarai, Japan
[4]Kyoto University, Kyoto, Japan

We report the discovery of a field-induced first-order phase transition at B^* within the superconducting state of UTe_2 under magnetic fields applied along the a-axis. This transition, observed in ultra-clean single crystals, is driven by a weak itinerant metamagnetic crossover in the normal-conducting state, originating from a Fermi surface instability associated with itinerant electron magnetism. Despite its subtle nature, this metamagnetism induces a sharp phase transition accompanied by a reconstruction of the superconducting order parameter, leading to a remarkable doubling of the upper critical field, B_{c_2}.

High-precision magnetocaloric effect and specific heat measurements reveal a distinct entropy jump at B^*, providing compelling evidence for a first-order phase transition within the superconducting state. We propose that this transition occurs between superconducting states of identical symmetry, where the balance between the A_u and B_{3u} components shifts abruptly. The strength of this scenario lies in its ability to consistently explain all experimental observations: 1) Since A_u is fully gapped and B_{3u} possesses point nodes, an increased B_{3u} weight naturally leads to a more anisotropic superconducting gap, accounting for the observed jump in entropy due to increased quasiparticle excitations. 2) The B_{3u} component, with spins aligned along the *a*-axis, gains Zeeman energy under magnetic fields applied parallel to this axis, thereby promoting a steeper slope of $B_{c_2}(T)$ and an overall increase in $B_{c_2}(0)$. 3) Remarkably, the observed clear phase transition is induced by a very weak metamagnetic crossover, which is fully consistent with our scenario where a shift in the order parameter components can, in principle, be triggered by infinitesimally small external perturbations.

Our study demonstrates the remarkable flexibility of multi-component superconductivity in adapting to subtle magnetic instabilities, offering new insights into the interplay between magnetism and unconventional superconductivity.

O19

5*f* electron occupancy and hybridization in the UTe_2 superconductor from XANES and XMCD studies.

Fabrice Wilhelm[1], Jean-Pierre Sanchez[2], Daniel Braithwaite[2], Georg Knebel[2], Gerard Lapertot[2], Andrei Rogalev[1]

[1]ESRF, Grenoble, France
[2]CEA, Grenoble, France

UTe_2 which is a newly discovered unconventional superconductor [1,2] has been investigated by x-ray absorption (XANES) and magnetic circular dichroism (XMCD) at the U- $M_{4,5}$ edges at 2.7 K at the ESRF ID12 beamline. The value of the branching ratio of the U- $M_{4,5}$ white lines confirms that the U ions are in an intermediate valence state between three (U^{3+}) and four (U^{4+}). The analysis of the XMCD data at the U-$M_{4,5}$ edges allows to conclude that the 5*f* electron count is about 2.8, *i.e.*, close to U^{3+}. Our finding agrees with other measurements (soft x-ray ARPES, core level photo- electron spectroscopy [3,4]) as well as with some band structure calculations [5,6]. This is an important conclusion. It invalids theoretical models promoting a dominant contribution of the $5f^2$ electronic configuration [7]. Furthermore, the reduction of the uranium orbital to spin magnetic moment ratio, compared to the free ion U^{3+} value, is a fingerprint of the 5*f* electron delocalization (hybridization). Another important breakthrough is the peculiar pressure dependence of the 5*f* electron count. We observe a decrease (increase) of about 0.2 e- of the 5*f* count (valence) at the transition at $P_c \approx 1.45$ GPa towards a magnetically ordered state [8]. This tiny change of the valence is accompanied by a modification of the electronic structure, a decrease of the magnetic anisotropy and the disappearance of the superconductivity. The decrease of the valence above 3 GPa could be due to a further change of the electronic structure associated with a structural transition. To conclude, it appears that the interplay between magnetism and valence instabilities is a key factor to understand the superconductivity in UTe_2. Our conclusions open the roads to further experiments under high pressure (XMCD, resistivity, x-ray or neutron diffraction) and theoretical models.

[1] S. Ran et al., Science 365, 684 (2019).
[2] D. Aoki et al., J. Phys. Soc. Jpn. 88, 043702 (2019).
[3] S.-I Fujimori et al., J. Phys. Soc. Jpn. 88, 103701 (2019).
[4] S.-I Fujimori et al., J. Phys. Soc. Jpn. 90, 015002 (2021).
[5] A. B. Shick and W. E. Pickett, Phys. Rev. B 100, 134502 (2019).
[6] A. B. Shick et al., Phys. Rev. B 103, 125136 (2021).
[7] L. Miao et al., Phys. Rev. Lett. 124, 076401 (2020).
[8] D. Aoki et al., J. Phys. Soc. Jpn. 89, 053705 (2020).

O20

Ultrasound Study of Field-Induced Superconducting Phases in UTe_2

Michal Vališka[1], Tetiana Haidamak[1], Andrej Cabala[1], Jiří Pospíšil[1], Vladimír Sechovský[1], Jan Prokleška[1], Andreas Hauspurg[2], Sergei Zherlitsyn[2]

[1]Charles University, Faculty of Mathematics and Physics, Department of Condensed Matter Physics, Prague, Czech Republic
[2]Hochfeld-Magnetlabor Dresden (HLD-EMFL), Helmholtz-Zentrum Dresden-Rossendorf, Dresden, Germany

Uranium ditelluride (UTe_2) is a prominent candidate for spin-triplet superconductivity, exhibiting a rich magnetic field–temperature phase diagram with multiple superconducting regions. Ultrasound velocity measurements were used to probe the elastic properties of UTe_2 under magnetic fields applied in the *b*-*c* crystallographic plane, up to 60 T. Clear anomalies in the sound velocity and elastic moduli were observed, corresponding to transitions between low-field and high-field superconducting states. In addition, a distinct feature near 15 T was identified, coinciding with anomalies previously reported in AC susceptibility measurements [1]. This additional phase boundary may indicate a change in the vortex structure or the emergence of a distinct superconducting state. The field and temperature dependence of the elastic response highlights the coupling between the lattice, magnetism, and superconductivity in UTe_2, providing further insight into the underlying mechanisms of its unconventional superconducting phases.

This work was supported by the Czech Science Foundation under the grant # 25-16339S

[1] H. Sakai, Y. Tokiwa, P. Opletal, M. Kimata, S. Awaji, T. Sasaki, D. Aoki, S. Kambe, Y. Tokunaga, and Y. Haga, Phys. Rev. Lett. 130, 196002 (2023).

O21

Unusual orders in $CeRh_2As_2$

Gertrud Zwicknagl

TU Braunschweig, Braunschweig, Germany. MPI-CPfS, Dresden, Germany

The heavy-fermion compound $CeRh_2As_2$ exhibits a complex phase diagram with rather unusual states at low temperatures. A prominent example is multi-phase superconductivity [1] which seems to develop inside a normal state whose order is still unclear. Thermodynamic and magnetic measurements seem to indicate a non-magnetic state with multipolar order, antiferromagnetic (AFM) order [2], however, was clearly detected by μSR and NQR/NMR experiments [3].

The present talk focusses on the instabilities of the strongly renormalized Fermi liquid state in the heavy-fermion compound $CeRh_2As_2$. The narrow quasiparticle bands which arise from the Ce-4f degrees of freedom via the Kondo effect are calculated by means of the Renormalized Band (RB) method. A simplified model band structure is used to calculate the momentum-dependent multipolar susceptibilities. We conjecture that the Kondo-induced quasi-quartet CEF ground state [4] in combination with pronounced nesting features of the Fermi surface [5] may give rise to ordered states involving multipolar degrees of freedom [2,6].

[1] S. Khim et al., Science 373, 1012 (2021).
[2] D. Hafner et al., Phys. Rev. X 12, 011023 (2022).
[3] S. Khim et al, Phys. Re.v B 111, 115134 (2025).
[4] D. Christovam et al, Physics Rev. Lett. 132, 046401 (2024).
[5] Yi Wu et al, Chinese Physics Letters 41, 097403 (2024).
[6] P. Khanenko et al, Phys. Rev. B 111, 045162 (2025).

O22

Magnetic Excitations of a Nodally-Hybridized Heavy-Fermion Semi-Metal: Application to CeNiSn

Peter Riseborough[1], Mucio Ciontinentino[2], Sergio Magalhaes[3], Luis Macedo[2]

[1]Temple University, Philadelphia, USA
[2]CBPF, Rio de Janeiro, Brazil
[3]Univ Fed Porto Alegre, Porto Alegre, Brazil

We examine the magnetic excitations of an Anderson Lattice Model with a V-shaped pseudogap due to nodal hybridization. The model produces a V-shaped pseudogap in the electron density of states close to the Fermi-Energy, similar to the low-temperature density of states inferred from NMR, break-junction and specific heat measurements on CeNiSn. CeNiSn has been described as a nodally hybridized semi-metal with a finite density of states in the pseudogap. The existence of low-dimensional Fermi-Surface has been inferred from measurements of Shubnikov-de Haas oscillations. The low-dimensional Fermi-surface has been attributed to the existence of metallic surface states, however, photoemission experiments indicate the existence of a quasi-one-dimensional Fermi-surface composed of bulk states. Inelastic neutron scattering experiments also show the existence of a spin-gap and unusual magnetic excitations. The interpretations of the experimental results are controversial. We hypothesize that the properties of CeNiSn could reflect a planar structure of nodes in the hybridization. The ALM model with nodal hybridization exhibits degenerate pairs of one-dimensional Fermi-surface located at the center of the pseudogap in accordance with the findings of photoemission experiments. At energies slightly off the Fermi-energy, the constant energy cuts develop into tori with small areas. We calculate the static and dynamic magnetic susceptibilities which show that the system exhibits distinct types of magnetic excitations that compare favorably with the experimentally observed spectra for CeNiSn. Analysis suggests that the dynamic exponent at the quantum critical point is z=1, which differs from the usual dynamic exponent z=2 found for a metallic antiferromagnetic quantum critical point. We also propose that the hypothesis of an anisotropic hybridization can be tested by tunneling spectroscopy at sites adjacent to substitutional impurities.

O23

Magnetic Phase Transitions in Sawtooth-Structured $CeRhSn_2$: Interplay of Frustration and Ordering?

P. Opletal[1], J. Fikáček[1], E. Duverger–Nédellec[1,2], A. Thamizhavel[3], Z. Hossain[4], D. legut[5], J. Custers[1]

[1]Charles University, Faculty of Mathematics and Physics, Department of Condensed Matter Physics, Prague, Czech Republic
[2]CNRS, ICMCB UMR5026, Bordeaux INP, Bordeaux University, F-Pessac CEDEX, France
[3]DCMP MS, Tata Institute of Fundamental Research, Mumbai, India
[4]Department of Physics, Indian Institute of Technology, Kampur, India
[5]IT4Innovations, VŠB-Technical University of Ostrava, Ostrava, Czech Republic

Low-dimensional magnetic materials continue to attract interest due to their unique electronic and magnetic properties. Recent studies suggest that the interplay among the Kondo effect, indirect magnetic interactions, and geometrical frustration in metallic systems can lead to complex phase behavior [1].

In this work, we present low-temperature experimental results on the Kondo lattice system $CeRhSn_2$, which features two inequivalent Ce sites arranged in sawtooth chains of alternating triangles. Prior investigations on polycrystals have revealed distinct magnetic ground states—either ferromagnetic (T_n = 4 K) or antiferromagnetic (T_n = 3.5 K) [2]. To clarify these findings, we synthesized single crystals and carried out magnetization (M), specific heat (C_p/T), and electrical resistivity (ρ) measurements.

Our results indicate an antiferromagnetic (AFM) transition at T_{m1} = 3.6 K, marked by a pronounced decrease in magnetization along the orthorhombic c-axis, a sharp discontinuity in C_p/T, and a kink in ρ. Upon further cooling, we observe a subsequent ferromagnet-like (FM) ordering at T_{m2} = 1.7 K, evidenced by a λ-shaped peak in C_p/T and a sudden resistivity drop. This lower transition exhibits hysteresis and shifts to higher temperatures under an applied magnetic field ($\mu_0 H$) along the b-axis, eventually merging with T_{m1} into a second-order FM transition. Additionally, a smaller λ-shaped anomaly emerges at lower temperatures, suggesting the presence of an additional magnetic phase.

Applying hydrostatic pressure (p) up to 3 GPa has minimal impact on transition temperatures—T_{m1} slightly increases, while T_{m2} remains largely unchanged. However, a new metastable transition appears above p > 0.4 GPa but is easily suppressed in a magnetic field. Neutron studies are necessary to further explore the various magnetic phases and the role of frustration in this system.

[1] M. W. Aulbach et al., Phys. Rev. B 92, 235131 (2019).
[2] Z. Hossain et al., J. Phys.: Condens. Matter 14, 9687 (2002).

O24

Quantum statistics near Mott localization: Superexclusion and distinguishability

Józef Spałek, Piotr Kuterba, Danuta Goc-Jagło, Maciej Fidrysiak

Institute of Theoretical Physics, Jagiellonian University, ul. Łojasiewicza 11, 30-348, Kraków, Poland

The appearance of Mott-Hubbard localization in nominally half-filled band systems is the signature of strong correlations of the respective electrons, where the Mott insulator state is that of Heisenberg antiferromagnet on the strong-correlation side. The associated principal question then is how to describe the electrons (or holes) in the vicinity of that singular state, particularly on that strong-correlation side. They do not form a Fermi liquid as their entropy (per carrier) in the high-temperature limit approaches the value $k_B \ln 2$, not $2k_B \ln 2$, as one would have for a Fermi liquid.

In the present work we propose to start from reciproacal (**k**) space description of those particles with the double occupancies $|\mathbf{k}\uparrow\downarrow>$ excluded in the **k** space. We call this extra feature the superexclusion, as it is additional to the ordinary Pauli exclusion. The model in the simplest situation can take the form of the Hubbard model in **k** space with the corresponding Hubbard parameter U increasing gradually to reach the strong-correlation regime [1,2,3]. Within this model we calculate the exact statistical distribution function $n_{\mathbf{k}\sigma}$ and the entropy, which reduces to that of the Mott insulator in the proper limit.

Furthermore, we consider the situation with spin-dependent particle mass in the spin-polarized situation [4,5] and argue that such particles are *distinguishable* in the quantum-mechanical sense, either in the Fermi-liquid state and that with the superexclusion.

Applicability of those concepts to real materials is briefly elaborated at the end. We also make a comparison of this new description with the results coming from either the Fermi-liquid or (introduced earlier) statistical spin-liquid picture.

This work is supported by Grants OPUS UMO-2021/41/B/ST3/04070 and UMO-2023/49/B/ST3/03545 from Narodowe Centrum Nauki (NCN).

[1] K. Byczuk and JS, Phys. Rev. B 51, 7934 (R) (1995).
[2] K. Jabłonowski et al., Phys. Rev. B 108, 195145 (2023).
[3] P.W. Philips et al., Nature Physics 16, 1175 (2020).
[4] JS and P. Gopalan, Phys. Rev. Lett. 64, 2823 (1990).
[5] JS, Physica B 378-380, 654 (2006).

O25

Variational framework for quantitative description of quantum collective excitations in correlated systems

Maciej Fidrysiak, Józef Spałek

Institute of Theoretical Physics, Jagiellonian University, Kraków, Poland

Multiple families of strongly correlated materials, ranging from transition metal oxides to *f*-electron heavy-fermion systems, exhibit pronounced collective excitations affecting their magnetic, charge, and superconducting properties in a unique manner. Yet, a unified microscopic description of local-correlation effects and long-wavelength magnetic/charge fluctuations remains a challenge due to their specific energy scales, as well as distinct temporal and spatial characteristics. To address those aspects, we have developed a theoretical framework combining variational wave function (VWF) approach with the field-theoretical expansion in the inverse number of fermionic flavors (1/*N*), in brief called VWF+1/*N* [1].

We outline the formulation of VWF+1/*N* approach and present calculated spin and charge susceptibilities for canonical correlated-electron models, encompassing Hubbard, *t*-*J*, and *t*-*J*-*U* Hamiltonians [2-4]. VWF+1/*N* provides a good agreement with static spin susceptibilities obtained from determinant quantum Monte Carlo simulations for the Hubbard model at weak coupling. Moreover, our approach allows for robust evaluation of dynamic properties and is capable of describing states with a spontaneously broken symmetry. The results are compared with those from resonant inelastic x-ray scattering (RIXS) experiments for high-temperature copper oxide superconductors, and semi-quantitative agreement is demonstrated for both paramagnon and acoustic plasmon spectra [5-6]. In particular, we theoretically account for the experimentally reported paramagnon persistence in wide range of doping. We also mention a recent application of VWF+1/*N* to infinite-layer nickelates [7], which exhibit a qualitatively distinct paramagnon dynamics despite their structural and electronic similarity to the cuprates. At the end, possible applications of our approach to microscopic models of *f*-electron heavy-fermion systems will be outlined.

This work is supported by Grants OPUS UMO-2021/41/B/ST3/04070 and UMO-2023/49/B/ST3/03545 from Narodowe Centrum Nauki.

[1] JS, MF, M. Zegrodnik, and A. Biborski, Phys. Rep. 959, 1 (2022).
[2] MF and JS, Phys. Rev. B 103, 165111 (2021).
[3] MF, D. Goc-Jagło, and JS, J. Magn. Magn. Mater. 539, 168395 (2021).
[4] MF, Acta Phys. Pol. A 143, 180 (2023).
[5] MF and JS, Phys. Rev. B 102, 014505 (2020).
[6] MF and JS, Phys. Rev. B 104, L020510 (2021).
[7] F. Rosa et al., Phys. Rev. B 110, 224431 (2024).

O26

Pressure-dependent Magnetism in 2D van der Waals Materials ($CrBr_3$ and VI_3): A Theoretical calculations

Krishna Kumar Pokhrel, Karel Carva, Suhasmita Ray

Charles University, Prague, Czech Republic

Two-dimensional (2D) van der Waals (vdW) materials have emerged as a rich platform for exploring novel quantum phenomena and next-generation device concepts. Among their many intriguing features, the recent discovery of magnetism in atomically thin layers [1] has opened new directions in spintronics and materials design.

Recent studies on $CrBr_3$ [2] have shown that the strength and even the sign of the interlayer magnetic exchange can vary significantly depending on how the layers are stacked. A similar tendency to form different magnetic phases under pressure has also been reported in VI_3 [3], highlighting a broader phenomenon across layered vdW magnets. These arguments suggest that both the phases with ferromagnetic (FM) and antiferromagnetic (AFM) interlayer interactions are present simultaneously in real samples, and their relative proportion depends on the pressure.

In this work, we investigate how applied pressure influences the magnetic properties of bilayer chromium bromide ($CrBr_3$) and vanadium triiodide (VI_3), two prominent 2D magnetic vdW materials. We present how pressure changes the magnetic coupling between layers, which is responsible for formation of different stacking configuration. To understand how these mixed-phase environments influence the magnetic transition temperature (T_C), we conducted finite-temperature Monte Carlo simulations using a stochastic Landau-Lifshitz-Gilbert (LLG) framework [4]. By modelling systems with varying proportions of AA and AB phase atoms—randomly distributed but differing in interlayer exchange—we quantify how the interplay between competing magnetic interactions shapes the thermal stability of magnetism under pressure.

[1] B. Huang et al., "Layer-dependent ferromagnetism in a van der Waals crystal down to the monolayer limit," Nature 546, 270–273 (2017).
[2] F.R. Yao et al., “Multiple antiferromagnetic phases and magnetic anisotropy in exfoliated $CrBr_3$ multilayers,” Nature Communications 14, 10 (2023), https://doi.org/10.1038/s41467-023-40723-x.
[3] P. Doležal et al., Crystal structures and phase transitions of the van der Waals ferromagnet VI_3 Physical Review Materials 3, 121401(R) (2019), https://doi.org/10.1103/PhysRevMaterials.3.121401.
[4] B. Skubic et al., A method for atomistic spin dynamics simulations: implementation and examples Journal of Physics: Condensed Matter 20, 315203 (2008), https://doi.org/10.1088/0953-8984/20/31/315203.

O27

Spin-glass and random-singlet ground-states in $NaCdM_2F_7$ pyrochlore (M = Co^{2+}, Ni^{2+}, Cu^{2+}) and defect-fluorite (M = Mn^{2+}) antiferromagnets

Andrej Kancko[1], Petr Proschek[1], Tetiana Haidamak[1], Cinthia Antunes Corrêa[2], Hironori Sakai[3], Yo Tokunaga[3], Marc Uhlarz[4], Adam Berlie[5], Ross Harvey Colman[1]

[1]Charles University, Faculty of Mathematics and Physics, Department of Condensed Matter Physics, Prague, Czech Republic
[2]Institute of Physics, Czech Academy of Sciences, Prague, Czech Republic
[3]Advanced Science Research Center, Japan Atomic Energy Agency, Tokai, Ibaraki, Japan
[4]Hochfeld-Magnetlabor Dresden (HLD), Helmholtz-Zentrum Dresden-Rossendorf, Dresden, Germany
[5]SIS Neutron and Muon Source, Didcot, United Kingdom

The family of $A'A''B_2F_7$ pyrochlore fluoride antiferromagnets represents a unique but understudied class of materials containing the 3D frustrated network of corner-sharing tetrahedra. While the rare-earth-based $A_2B_2O_7$ pyrochlore oxide counterparts have long been the main focus of study for their exotic magnetic ground states (spin glass, spin ice, spin liquid, order-by-disorder etc.), studies of these systems require extremely low temperatures due to the weak dipolar interactions between the magnetic 4f ions ($|\theta_{CW}| \sim 10^0 - 10^1$ K).

Conversely, the $A'A''B_2F_7$ pyrochlore fluorides [1] overcome this limitation by replacing oxygen (O^{2-}) with fluorine (F^{1-}), enabling the stabilization of divalent magnetic 3d-transition-metal ions (from Mn^{2+} to Cu^{2+}) with stronger super-exchange interactions ($|\theta_{CW}| \sim 10^1 - 10^2$ K) on the pyrochlore B-site. Charge balancing and structure stability constraints, however, require a mixed occupancy of the pyrochlore A-site by monovalent A'^{+} and divalent A''^{2+} cations, leading to chemical disorder, which consequently introduces magnetic bond disorder due to the A'^{+}/ A''^{2+} ionic size mismatch.

In our contribution, we report the successful synthesis and magnetic characterisation of novel frustrated $NaCdM_2F_7$ pyrochlore (M = Co^{2+}, Ni^{2+}, Cu^{2+}) and defect-fluorite (M = Mn^{2+}) antiferromagnets. [2,3] While M = Co^{2+} (J_{eff} = ½), Ni^{2+} (S = 1) and Mn^{2+} (S = 5/2) indicate a frozen spin-glass-like ground-state at $T_f \sim 2 - 4$ K by means of AC susceptibility measurements, M = Cu^{2+} (S = ½) shows no magnetic transition in magnetisation or specific heat, with continued spin dynamics down to 50 mK confirmed by μSR and NMR measurements, hinting the realisation of a quantum spin liquid ground-state. In addition, $NaCdCu_2F_7$ shows a power-law scaling of low-temperature susceptibility $\chi(T) \sim T^{-\gamma}$ (with $\gamma = 0.68$), as well as data collapse of magnetic specific heat $(\mu_0 H)^{\gamma} C_{mag}/T$ *vs.* $T/\mu_0 H$ and isothermal magnetization $MT^{\gamma-1}$ vs. $\mu_0 H/T$. This suggests random-spin-singlet physics stemming from spins with a power-law distribution of exchange energies $P[J] \sim T^{-\gamma}$. [4]

[1] D. Reig-i-Plessis and A. M. Hallas, Phys. Rev. Mater. 5, 030301 (2021).
[2] A. Kancko, G. Giester and R. H. Colman, Phys. Scr. 98, 075947 (2023).
[3] A. Kancko, C. A. Corrêa and R. H. Colman, J. Alloys Compd. 1024, 180142 (2025).
[4] I. Kimchi et al., Nat. Commun. 9, 1 (2018).

O28

Measurement of Altermagnetic Magnon Splitting in CrSb with Circularly Polarized X-Ray Scattering

Nikolaos Biniskos[1,2], Manuel dos Santos Dias[3], Stefano Agrestini[4], David Sviták[1], Ke-Jin Zhou[4], Jiří Pospíšil[1], Petr Čermák[1]

[1]Charles University, Prague, Czech Republic
[2]Institute Laue Langevin, Grenoble, France
[3]STFC Daresbury Laboratory, Warrington, United Kingdom
[4]Diamond Light Source, Didcot, United Kingdom

Altermagnets constitute a newly identified class of compensated antiferromagnets whose magnetic sublattices break time-reversal symmetry in a nonrelativistic manner, combining features of both ferromagnets and antiferromagnets. Although their unique electronic signatures – such as anomalous Hall effects and X-ray magnetic circular dichroism – have been demonstrated, direct experimental access to their fundamental collective excitations, magnons, has remained elusive. Magnons not only mediate spin transport in magnonic devices but also encode the symmetry-breaking that defines altermagnetism; resolving their energy spectrum and polarization is key to both fundamental understanding and future applications in low-power spintronics.

Here we present a **novel measurement protocol** leveraging resonant inelastic X-ray scattering (**RIXS**) with circularly polarized photons to directly probe magnon chirality in the metallic altermagnet CrSb [1]. Using high-resolution RIXS, we measured magnon excitations with both right- and left-hand circular polarizations. By focusing the X-ray beam onto individual altermagnetic domains and performing azimuthal rotations of the sample, we isolated the circular dichroism of the magnon peaks, an unambiguous fingerprint of their chiral character.

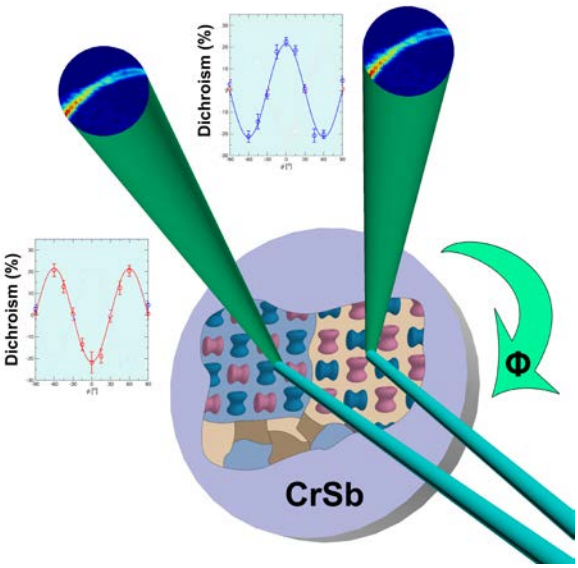

Our measurements reveal a dispersive magnon branch in agreement with theory. Crucially, **we observe** a pronounced **circular-dichroic asymmetry** of up to 20 % for magnon peaks at off-symmetry wavevectors, which reverses sign upon either inversion of the in-plane momentum or switching to a different antiferromagnetic domain. The azimuthal dependence follows a cos functional form, matching the predicted angular modulation of the altermagnetic magnon splitting. Although the two split branches lie within our energy resolution, the dichroic intensity provides a robust proxy for their chiral nature.

This work constitutes the **first direct mapping** of circularly polarized magnon modes in an altermagnet and establishes RIXS-based magnetic circular dichroism as a powerful, domain-resolved probe of altermagnetic order. By bridging theoretical predictions and experimental observables, our protocol opens new avenues for the exploration of altermagnetic magnonics and for the design of hybrid spintronic devices that exploit chiral spin-wave transport.

[1] Biniskos, Nikolaos, et al. "Systematic Mapping of Altermagnetic Magnons by Resonant Inelastic X-Ray Circular Dichroism." *arXiv preprint arXiv:2503.02533* (2025).

O29

Novel Fission Track Detector for Nuclear Forensics: Integrated Aerogel-Lexan detector to determine the different fission isotope

Itzhak Halevy[1], Rami Babayew[1,2], Yaacov Yehuda-Zada[3], Galit Bar[4], Noam Elgad[2,1], Mark Last[5], Jan Lorincik[6], Itzhak Orion[1], Shay Dadon[3], Aryeh Weiss[7], Galit Katarivas Levy[8]

[1]Unit of Nuclear Engineering, Faculty of Engineering Sciences, Ben Gurion University, Beer-Sheva, Israel
[2]Engineering Department, Nuclear Research Center Negev, Beer-Sheva, Israel
[3]Nuclear Research Center Negev, Beer-Sheva, Israel
[4]Department of Solid-State Physics, Soreq Nuclear Research Center, Yavne, Israel
[5]Department of Software and Information Systems Engineering, Ben Gurion University, Beer-Sheva, Israel
[6]Nuclear Fuel Cycle Department, Centre Řež, Husinec, Czech Republic
[7]Bar Ilan University, Ramat Gan, Israel
[8]Department of Biomedical Engineering, Ben-Gurion University, Beer-Sheva, Israel

Fission Track Analysis (FTA) is a pivotal tool in nuclear forensics, enabling identification and characterization of nuclear materials by examining fission fragment tracks in Solid-State Nuclear Track Detectors (SSNTDs). This study enhances FTA precision by introducing a novel detector design integrating Aerogel material and advanced image processing developed in MATLAB.
Literature shows each fissile isotope exhibits a unique fission product yield. We propose that beyond identifying fissile particles, FTA can also reveal isotopic characteristics based on fission track length distributions.

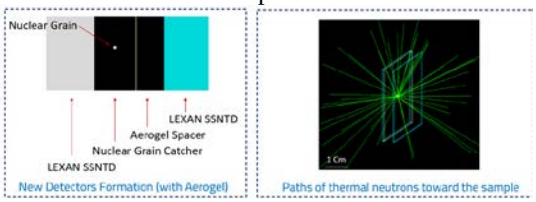

Fig. 1. Setup configuration in Geant4

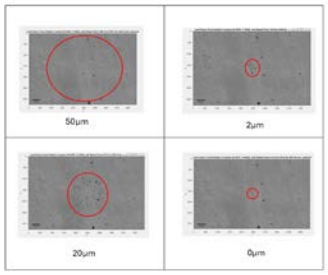

Fig. 2. The same particle U-235 size in different Aerogel thicknesses.

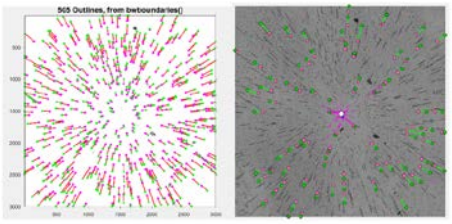

Fig. 3. Image Processing on simulated fission track on SSNTD with 50µm Aerogel

Monte Carlo simulations performed using GEANT4 (v10.6) with the QGSP_BERT_HP physics list to model fission product trajectories. Synthetic fission track clusters were generated using the FTA TRAINER 2.4 [1], overlaying simulated tracks onto real SSNTD backgrounds. These datasets supported the development and validation of image processing algorithms for pattern analysis and property reconstruction. We validated the algorithms using both synthetic datasets and real fission tracks from the IAEA314 reference material. Synthetic data enabled controlled development, while real images tested robustness under realistic conditions.

Analysis of U-235 Natural Enrichment **Real** and **Simulated** Cluster:

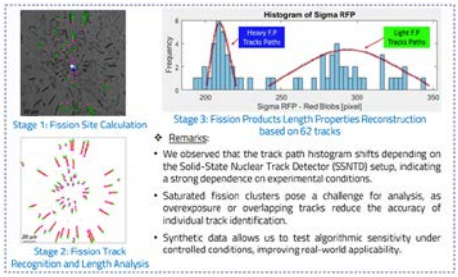

Fig. 4. Image Processing on **simulated** fission cluster

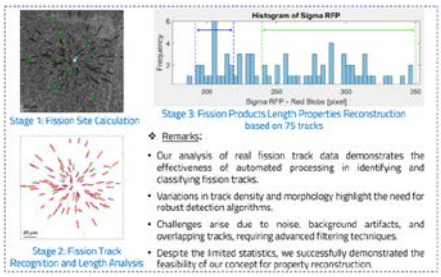

Fig. 5. Image Processing on **Real** Data on reference material IAEA 314

Key Result:
Using GEANT4 datasets of Th-229, U-233, and U-235, image processing with Aerogel spacers revealed distinct histogram peak centers, supporting the concept of isotope differentiation through improved FTA.

[1] R. Babayew, Y. Yehuda-Zada, N. Elgad, J. Lorince, I. Orion, A. Weiss, G. Katarivas Levy, I. Halevy, **Simulation tools for improvement of the fission track analysis method for nuclear forensics** (2024), JRNC, Akadémiai Kiadó, Budapest, Hungary, DOI: 10.1007/s10967-023-09313-5.

O30

Transforming Healthcare through Additive Manufacturing

Galit Katarivas Levy

Ben-Gurion University of the Negev, Beer Sheva, Israel

Additive manufacturing (AM) is transforming the landscape of modern healthcare by enabling personalized, patient-specific solutions that directly address clinical challenges. At the GKLab for Advanced Biomaterials and AM, we harness advanced multi-material 3D printing technologies to pioneer medical applications that go beyond conventional treatment paradigms. Our work integrates engineering innovation with clinical insight to improve therapeutic outcomes, reduce surgical risks, and restore patient quality of life. In this talk, I will present two projects that highlight the transformative power of AM in patient care. The first project involves hybrid therapeutic garments for scar management, designed for individuals with hypertrophic and keloid scars. These garments integrate biocompatible, FDA-approved elastic materials with personalized compression and hydration layers, all printed directly onto textiles. Developed in collaboration with clinicians and tailored to each patient's anatomy and preferences, they enhance comfort, aesthetics, and treatment adherence. The second project, FemiNip, addresses the unmet needs of breast cancer survivors who have undergone mastectomy but cannot or choose not to pursue surgical reconstruction or tattooing. By using high-resolution scanning and multi-material printing, we create hyper-realistic, patient-specific nipple and areola prostheses that restore physical appearance and support emotional healing through a culturally sensitive, non-invasive solution. Together, these innovations exemplify how additive manufacturing can serve as a powerful enabler of compassionate, customized healthcare.

O31

Magnetic and quadrupole coupling emerging in NdB_4 with geometrical frustration

Naoto Metoki

Ibaraki University, Mito, Japan

NdB_4 with frustrated orthogonal AFM dimers on Shastry-Sutherland lattice [Fig. 1(a),(b)] shows a successive magnetic order [1,2].
(1) In-plane moment $m_\perp(\boldsymbol{q_0})$ with 'All-in All-out' structure below T_0 = 17.2 K [Fig. 1(c)], accompanying a weak secondary order parameter of c-moment $m_c(\boldsymbol{q_0})$ [Fig. 1(d)] with an induced type temperature dependence (Fig. 2), where $\boldsymbol{q_0}$ = (0,0,0).
(2) Spontaneous long-period modulations of m_c with $\boldsymbol{q_{s1}}$=(0.14,0.14,0.4) and $\boldsymbol{q_{s2}}$=(0.2,0,0.4) below T_{N1} = 6.8 K and T_{N2} = 4,9 K, respectively.

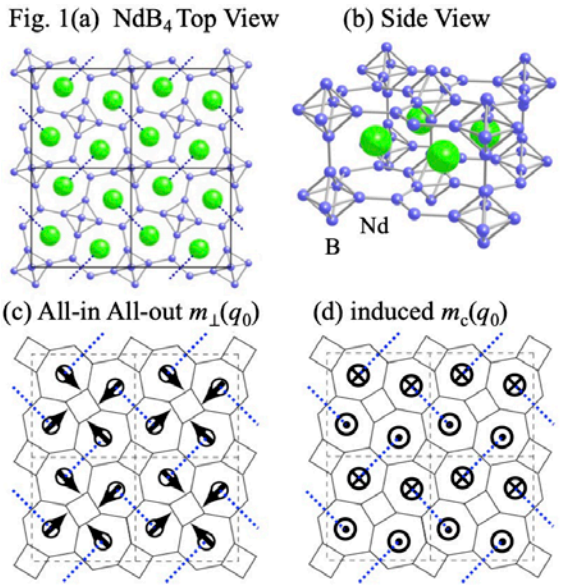

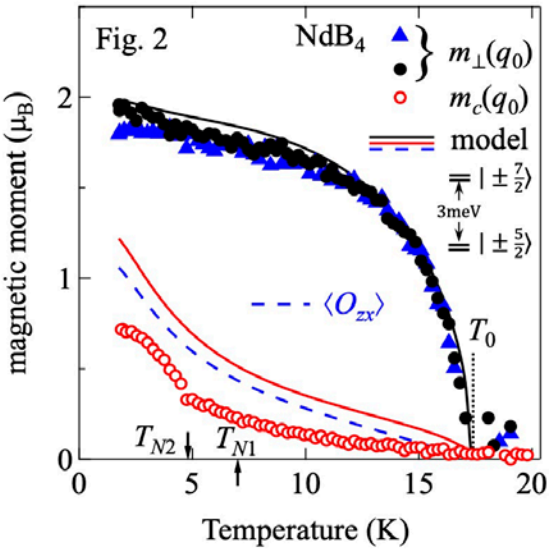

The unusual order of (1) $m_\perp(\boldsymbol{q_0})$ and $m_c(\boldsymbol{q_0})$ is understood based on the pseudo quartet with the ground state of $|\pm5/2\rangle$ and $|\pm7/2\rangle$ at ΔE = 3 meV, clarified in our neutron scattering study [3]. This f electron state comes from a uniaxial and in-plane isotropic CEF potential H_{CEF} from Boron heptagons. The pseudo quartet splits and mixed into four levels in the ordered states by the on-site Hamiltonian $H = H_{CEF} + H_M + H_K$, where $H_M = A{\cdot}J_x \langle J_x\rangle$ is the magnetic interaction and $H_K = K{\cdot}J_x\, O_{zx} \langle J_x\rangle$ denotes the coupling of magnetic J_x and quadrupole O_{zx}. The excitation spectra are well explained with this model and the order parameters $m_\perp(\boldsymbol{q_0}) = g_j \langle J_x\rangle$ and $m_c(\boldsymbol{q_0}) = g_j \langle J_z\rangle$ are reproduced as shown in Fig. 2. The temperature dependence of $\langle O_{zx}\rangle$ is very similar to that of $m_c(\boldsymbol{q_0})$ [4].
The frustration is somehow broken by weak interactions such as long-range, higher-order, quadrupole, and their coupling. They are usually negligible but dominate having casting vote for the unusual ordered states under geometrical frustrations, where the strong Heisenberg interactions are canceled out.
H_K derived as $\sim J_z \langle J_x\rangle$ is equivalent to the coupling of in-plane and out-of-plane components. Dzyaloshinskii-Moriya interaction (DMI) given by vector cross products contains J_zJ_x, but we found DMI not energetically contributing to $m_c(\boldsymbol{q_0})$. The third term of exchange interaction having symmetric tensor form may attribute to $m_c(\boldsymbol{q_0})$. But this term of forth-order perturbation is expected to be very small.
The successive magnetic and quadrupole order of NdB_4 is very similar to those of NpTGa$_5$ presented at the 7th Prague colloquium in 2004. No induced secondary order parameter in NpTGa$_5$ may attribute to the absence of geometrical frustration.

[1] H. Yamauchi et al., J. Phys. Soc. Jpn., 86, 044705 (2017).
[2] N. Metoki et al., Phys. Rev. B 97, 174416 (2018).
[3] H. Yamauchi et al., J. Phys. Soc. Jpn., 94, 054705 (2025).
[4] N. Metoki et al., Phys. Rev. B 111, 104424 (2025) (Editor's suggestion).

O32

Utilizing frustration in Gd- and Yb-based oxides for milli-Kelvin adiabatic demagnetization refrigeration

Tim Treu[1], Prachi Telang[1], Marvin Klinger[1], Christian Heil[1], Alexander Tsirlin[2], Anton Jesche[1], Philipp Gegenwart[1]

[1]University of Augsburg, Augsburg, Germany
[2]University of Leipzig, Leipzig, Germany

Gadolinium- and Ytterbium-oxide based frustrated magnets have recently been characterised as excellent millikelvin adiabatic demagnetization refrigerants [1]. They offer several advantages over conventional paramagnetic hydrated salts, which have traditionally been employed for milli-Kelvin adiabatic demagnetization refrigeration (mK-ADR). For example these novel ADR materials enable cooling to temperatures several times lower than the magnetic interaction strength, significantly enhancing the entropy density and cooling power at a given target temperature. A further advantage is their chemical stability, allowing for a much simpler ADR pill design and ultra-high vacuum applications.

We present a comprehensive study of the structural, magnetic and thermodynamic properties as well as the adiabatic demagnetisation refrigeration performance of several different Gd- and Yb-based oxides (including [1-2] and further unpublished results). For the temperature range between 0.03 and 2 K, a systematic comparison of the field-induced entropy density change and the refrigerant capacity is provided, demonstrating the advantages of frustrated magnets for low temperature ADR.

[1] T. Treu et al., J. Phys. Condens. Matter 37, 013001 (2025).
[2] P. Telang et al., Phys. Rev. B 111, 064431 (2025).

O33

Magnetoelectric Coupling and Dielectric Anomalies in the Frustrated Quantum Magnet $PrMgAl_{11}O_{19}$

Sonu Kumar[1,2], Petr Proschek[1], Ross Colman[1], Maxim Savinov[3], Stanislav Kamba[3], Gael Bastien[1]

[1]Department of Condensed Matter Physics, Charles University, Prague, Czech Republic
[2]Department of Physics of Experimental Condensed Matter, Faculty of Physics and Astronomy, Adam Mickiewicz University, Poznan, Poland
[3]Institute of Physics, Czech Academy of Sciences, Prague, Czech Republic

The interplay of magnetic and electric degrees of freedom in frustrated quantum magnets enables the emergence of exotic phases and magnetoelectric effects. We present a dielectric spectroscopy study of the non-Kramers rare-earth compound $PrMgAl_{11}O_{19}$, investigating its magnetoelectric properties from 0.3 K to 300 K under magnetic fields up to 9 T. Below 5 K, the dielectric constant deviates from the quantum paraelectric Barrett formula, exhibiting an anomaly that parallels Schottky-like features in specific heat data [1]. This anomaly, driven by low-lying excitations from two distinct Pr^{3+} sites, shifts with applied magnetic fields, indicating robust magnetoelectric coupling. A two-gap model, inspired by our prior thermodynamic work [1], captures the dielectric response's qualitative shape and field dependence, though fitted gap values differ from those in specific heat. The electric dipoles, arising from Al^{3+} displacements within AlO_5 bipyramids [2], underscore the spin-lattice interactions in this triangular lattice magnet. These results suggest that a more sophisticated theoretical framework is needed to unify dielectric and thermodynamic observations in $PrMgAl_{11}O_{19}$.

[1] S. Kumar et al., "Induced quantum magnetism on a triangular lattice of non-Kramers ions in $PrMgAl_{11}O_{19}$." https://arxiv.org/pdf/2410.07885.
[2] J. Li et al., "Structural studies of $CaAl_{12}O_{19}$, $SrAl_{12}O_{19}$, $La_{2/3+\delta}Al_{12}O_{19-\delta}$, and $CaAl_{10}NiTiO_{19}$ with the hibonite structure; indications of an unusual type of ferroelectricity," Zeitschrift fur Naturforschung - Section B Journal of Chemical Sciences, vol. 71, no. 5, pp. 475–484, (2016).

O34

Electronic Properties of Eu-Based Compounds under High Pressure

Fuminori Honda[1], Yoshichika Onuki[2]

[1]Central Institute of Radioisotope Science and Safety, Kyushu University, Fukuoka, Japan
[2]CEMS, RIKEN, Wako, Japan

The valence state of europium (Eu) is known to be highly sensitive to external pressure, providing a unique platform to explore pressure-induced electronic and magnetic phenomena. Based on systematic studies, we have proposed that Eu-based compounds under pressure can be broadly classified into three types of pressure-temperature (P-T) phase diagrams. The first type is the well-known pressure-induced valence transition (PIVT), exemplified by $EuRh_2Si_2$, where Eu exhibits a gradual change from a divalent to a mixed-valent state with increasing pressure [1,2]. The second is the Doniach-type behavior, as seen in $EuPt_2Si_2$, which resembles the heavy-fermion behavior of Ce-based compounds [1-3]. In this case, magnetic ordering is progressively suppressed with increasing pressure and disappears around 4 GPa. The third type is characterized by a sharp valence crossover, as observed in $EuCu_2Ge_2$ [4] and $EuPt_3Al_5uPt_3Al$ and EuPt and EuPt characterized by a sharp valence crossover, as observe P_c. Since the system exhibits critical behavior at P_c and crossover-like resistivity above it, this suggests a change in the electronic state accompanied by a small but distinct shift in the Eu valence.

To further investigate these behaviors, we have synthesized high-quality single crystals of several Eu-based compounds and performed extensive pressure-dependent measurements. We highlight our recent findings on $EuRu_2Ge_2$, which shows ferromagnetic ordering at T_C = 61 K at ambient pressure, followed by a valence transition above 4.0 GPa. In contrast, $EuGa_4$ exhibits minimal valence change up to 20 GPa, despite earlier suggestions of PIVT behavior [1]. $EuRu_2P_2$ shows a gradual valence change beginning around 2 GPa, with temperature-dependent valence states appearing at higher pressures (~13 GPa). In this presentation, we will discuss the diverse responses of these Eu-based systems to pressure, with an emphasis on their electronic and magnetic states.

[1] Y. Onuki et al., J. Phys. Soc. Jpn. 89, 102001 (2020) and references therein.
[2] F. Honda, Physica B 536, 182 (2018).
[3] T. Takeuchi et al., J. Phys. Soc. Jpn. 87, 074709 (2018).
[4] J. Gouchi, Phys. Soc. Jpn. 89, 053703 (2020).
[5] T. Koizumi et al., J. Phys. Soc. Jpn. 91, 043704 (2022).

O35

Perpendicular magnetic anisotropy in a single Dy adatom ferrimagnet

Dominik Legut[1,2], Frantisek Maca[3], Itzak Halevy[4], Alexander Shick[3]

[1]Charles University, Prague, Czech Republic
[2]VSB Technical University of Ostrava, Ostrava, Czech Republic
[3]Academy of Sciences of the Czech Republic, Prague, Czech Republic
[4]Ben Gurion University of Negev, Beer-Sheva, Israel

The electronic structure and magnetism of individual Dy atoms adsorbed on ferromagnetic (Gr)/Ni(111) substrate are investigated using a combination of the density functional theory with the Hubbard-I approximation to the Anderson impurity model (DFT+U(HIA)). The divalent Dy^{2+} adatom in f^{10} configuration with [J = 8, L = 6, S = 2] is found. The values of spin M_S =3.4 μ_B, orbital M_L=5.2 μ_B, and total M_J =8.6 μ_B calculated for the Dy f-shell are noticeably different from the atomic second Hund's rule. There is almost zero moment on (Gr)-atoms. The ferromagnetic Ni substrate moments are anti-aligned to the Dy 4f-shell moment. The X-ray absorption (XAS) and magnetic circular dichroism (XMCD) spectra are calculated and can be compared to the experi- mental data. The magnetic anisotropy energy (MAE) is calculated from the ground state energy difference for different directions of the magnetization, E[100] - E[001] = 2.8 meV and E[010] - E[001] = 2.2 meV. This large and positive MAE can be important for ultra-high density magnetic recording. The magnetization of Dy@(Gr)/Ni(111) is tilted with respect to the (Gr)/Ni(111) substrate-normal by 38º due to a competition between negative first and third order magnetic anisotropies and strong and positive second order magnetic anisotropies. Our studies assist in resolving ambiguities of conventional DFT+U applied to Dy on graphene. They can provide a viable route for further investigation and prediction of the rare-earth based magnetic nanostructures.

P01

Angle-Resolved Photoemission Spectroscopy Study of Kondo Semimetals/Insulators: CeNiSn, CeRhSb, CeRhAs

J.-S. Kang[1], Seungho Seong[1], J. D. Denlinger[2], T. Takabatake[3], Y. Onuki[4], B. I. Min[5]

[1]The Catholic University of Korea, Bucheon, Republic of Korea
[2]Lawrence Berkeley National Laboratory, Berkeley, USA
[3]Hiroshima University, Higashi-Hiroshima, Japan
[4]RIKEN, Wako, Japan
[5]POSTECH, Pohang, Republic of Korea

The recent theoretical prediction of the topological Kondo insulators (TKIs) of Ce-based ternary compounds [1,2], such as CeNiSn, CeRhSb, and CeIrSb, has triggered the revived attention to the Kondo insulators and Kondo semimetals. The predicted TKI properties of CeNiSn, CeRhSb, and CeIrSb arise from the strong spin-orbit coupling and the odd parity of the f-electron states[1,2]. A unique feature of these systems is the nonsymmorphic glide and screw axis symmetries that bring about the new topological surface states and the hour-glass type bulk band structures. Despite extensive work on the possible TKI candidate materials, the TKI nature of their electronic structures has not been confirmed experimentally yet. In this work, we have investigated the electronic structures of isostructural CeNiSn, CeRhSb, and CeRhAs employing angle-resolved photoemission spectroscopy (ARPES). CeNiSn and CeRhSb were known as the Kondo semi-metals with large anisotropy in resistivity for a long time [3], and isostructural CeRhAs was known as the Kondo insulator. In this work, we have performed temperature (T)-dependent APPES measurements, from which we have investigated the T-dependence of the Ce 4f states and determined their Kondo temperatures. This work demonstrates the importance of the coherent Kondo states in determining the potential topological properties of CeNiSn, CeRhSb, and CeRhAs.

[1] M. Dzero, J. Xia, V. Galitski, and P. Coleman, Annu. Rev. Condens. Matter Phys. 7, 249 (2016).
[2] Po-Yao Chang, O. Erten, P. Coleman, Nat. Phys. 13, 794 (2017).
[3] T. Takabatake, et al., Phys. Rev. B. 50, 623 (1994).

P02

Magnetic properties of the $Dy_xY_{1-x}(PO_3)_3$ glasses

Vladimír Tkáč[1], Vladyslav Stadnyk[1], Martin Tokarčík[1], Róbert Tarasenko[1], Erik Čižmár[1], Pavlo Baloh[2], Martin Orendáč[1], Alžbeta Orendáčová[1], Jana Holubová[3], Eva Černošková[3], Zdeněk Černošek[3], Alexander Feher[1]

[1]Institute of Physics, Faculty of Science, P. J. Šafárik University in Košice, Park Angelinum 9, 041 54, Košice, Slovakia
[2]International Institute for Carbon-Neutral Energy Research, Kyushu University (I2CNER), 744 Motooka, Nishi-ku, 819-0395, Fukuoka, Japan
[3]Department of General and Inorganic Chemistry, Faculty of Chemical Technology, University of Pardubice, Studentská 573, 532 10, Pardubice, Czech Republic

The magnetic properties of rare-earth ions are mainly studied in the periodic and symmetrical crystal structures. The influence of the crystal-electric field (CEF), which surrounds the magnetic ions in such cases, is mainly identical for every magnetic ion.

We performed the experimental study of the magnetic properties of the $Dy_xY_{1-x}(PO_3)_3$ glassy system with several concentrations of Dy^{3+} ions, x = 0, 0.0001, 0.001, 0.01, 0.1, and 1. The excess over the Debye contribution, called the boson peak, characterizes the specific heat C_p of the non-magnetic sample (x = 0) at $T_{BP} \approx 12$ K [1], which is typical for the amorphous material. Additional magnetic contributions are observed in the magnetic samples ($x \neq 0$), revealed as an onset of Shottky maximum in the x = 1 sample [1]. The magnitude of the maximum decreases with the decreasing content of the magnetic ions. The external magnetic field application shifts the Shottky maximum to higher temperatures, which is connected with reducing the magnitude.

The magnetization measurements showed that saturated magnetization was lower than the expected saturation value $\mu_{eff} = 10.65\mu_B$ at T = 1.8 K due to the strong anisotropy of the Dy^{3+} ions. Magnetic susceptibility measurements between T = 1.8 K and 300 K in the temperature range revealed no difference between zero field cooling and field cooling regimes, indicating the absence of magnetic phase transitions. The fitting procedure using Curie-Weiss law showed weak antiferromagnetic interactions, which decrease with lowering Dy^{3+} concentrations. The effective magnetic moment at T = 300 K indicates values close to $\mu_{eff} = 10.65\mu_B$.

AC susceptibility experimental study revealed the presence of slow magnetic relaxation in zero magnetic field characterized by the presence of one relaxation process. The relaxation process slows down with decreasing magnetic concentration. Sample with x = 1 relax above f = 10 kHz, x = 0.1 at f = 3000 Hz, x = 0.01 at f = 730 Hz, x = 0.001 at f = 20 Hz and x = 0.0001 below f = 0.1 Hz. This may be caused by the weakening of the magnetic interactions between Dy^{3+} ions.

Acknowledgements

The work was supported by the project APVV-22-0172.

[1] P. Baloh et al., Thermodynamic properties of the phosphate glass $Dy(PO_3)_3$ – Potential influence of boson peak on spin relaxation, J. Magn. Magn. Mater. 588 171415 (2023).

P03

Magnetism of $Nd_{3-x}U_xRu_4Al_{12}$ intermetallic compounds

A. Andreev[1], D. Gorbunov[2], J. Šebek[1]

[1]Institute of Physics, Academy of Sciences, Prague, Czech Republic
[2]Hochfeld-Magnetlabor (HLD-EMFL), Dresden, Germany

The ternary intermetallic compounds $R_3Ru_4Al_{12}$ (R – rare-earth element or U) crystallize in a hexagonal crystal structure of $Gd_3Ru_4Al_{12}$ type (space group $P6_3/mmc$). It was found that $Nd_3Ru_4Al_{12}$ is a ferromagnet and displays uniaxial anisotropy, whereas its actinide analog, $U_3Ru_4Al_{12}$, is an antiferromagnet and shows planar anisotropy. Therefore, the single-ion and two-ion mechanisms lead to distinct anisotropies. We prepared $Nd_{3-x}U_xRu_4Al_{12}$ single crystals (x = 0, 1, 2, 3) in order to study the evolution of their magnetic properties. The crystals were grown by the modified Czochralski method in a tri-arc furnace. The lattice of $Nd_{3-x}U_xRu_4Al_{12}$ shrinks with x anisotropically (by 0.4% in basal plane and by 2.1% along the [001] axis).

Magnetization curves show that $Nd_3Ru_4Al_{12}$ is a ferromagnet (below T_C = 39 K) with easy axis [001]. A strong uniaxial magnetic anisotropy (the first anisotropy constant is 3 MJ m^{-3} at 2 K) leads to a large magnetic hysteresis (m_0H_c = 2 T at 2 K) of narrow domain walls. The anisotropy within the basal plane is not large, nevertheless, it is non-negligible, the [120] axis is the hardest magnetization axis. For $x \geq 1$, $Nd_{3-x}U_xRu_4Al_{12}$ do not show spontaneous magnetization, therefore, they are not ferromagnets. For the materials with x = 1 and 2, we did not find any anomaly in the magnetic susceptibility as a function of temperature. Therefore, $Nd_2URu_4Al_{12}$ and $NdU_2Ru_4Al_{12}$ are likely paramagnets. The U substitution for Nd affects also the magnetic anisotropy. For x = 1, the strong uniaxial anisotropy is still observed, whereas the compound with x = 2 is close to magnetically isotropic below 14 T. Finally, the magnetization becomes larger in the basal plane than along the [001] axis at x = 3, confirming a basal-plane arrangement of its antiferromagnetic structure.

The effective magnetic moment, μ_{eff}, per R atom is 3.6 μ_B at x = 0. With increasing x, μ_{eff} decreases to 2.5 μ_B. The difference in the paramagnetic Curie temperatures, θ_p, between the [100] axis and the basal plane is 45 K at x = 0, which confirms the strong uniaxial anisotropy seen from magnetization curves. At x = 3, this difference is -28 K. The anisotropy is of the easy-plane type and is weaker in magnitude than for x = 0. A change of the anisotropy type occurs in the vicinity of x = 2, in accordance with M vs. H data.

P04

Pseudogap in slightly doped $Y_{0.77}Pr_{0.23}Ba_2Cu_3O_{7-\delta}$ single crystals

Liudmyla Bludova[1], Ahmed Sedda[2], Erkki Lähderanta[2], Ruslan Vovk[3], Andrei Solovjov[1]

[1]B.Verkin Institute for Low Temperature Physics and Engineering of NAS of Ukraine, Kharkiv, Ukraine [2]Lappeenranta University of Technology, Lappeenranta, Finland
[3]V. Karazin Kharkiv National University, Kharkiv, Ukraine

The pseudogap (PG) state, which is opened in cuprate high-temperature superconductors (HTSCs) below the characteristic temperature $T^* >> T_c$, is one of the most mysterious and simultaneously interesting phenomena in modern solid state physics [1]. It is well established that in HTSCs, the PG is observed when the charge carrier concentration varies between slightly doped (SD) and optimally doped levels. Understanding the PG physics would definitely shed more light on the mechanism of superconducting pairing in HTSCs, which is also not fully clarified yet. The $YBa_2Cu_3O_{7-\delta}$ cuprate is believed to be the most reliable material for studying the PG [1], especially when high pressures is applied [2, 3].

In our work, for the first time, we carried out the analysis of the influence of hydrostatic pressure up to 1.1 GPa on the temperature dependence of pseudogap $\Delta^*(T)$ of the SD $Y_{0.77}Pr_{0.23}Ba_2Cu_3O_{7-\delta}$ single crystals. It is shown that the pressure effect on T_c and resistivity $\rho(T)$ is different. Under pressure $\rho(T)$ decreases, while T_c increases, which is associated with the redistribution of charge carriers in the CuO_2 planes. It was shown that under pressure the $\Delta^*(T)$ increases with a rate $d\ln\Delta^*/dP = 0.9\ GPa^{-1}$, which is most likely due to a decrease in the frequencies of the phonon spectrum of the superconductor when pressure is applied. It is revealed that without pressure, a “magnetic” maximum occurs on the $\Delta^*(T)$ at high temperatures, followed by a linear section with a positive slope, limited by the temperatures of structural transition T_S and spin density wave ordering T_{SDW}. At P = 1.1 GPa the maximum disappears (Fig.1). The transition of $\Delta^*(T)$ into the superconducting state below the temperature T_{01}, that limits the superconducting fluctuations from above, happens in a usual way.

[1] A.L. Solovjov, V.M. Dmitriev, Low Temp. Phys. 32, 576 (2006).
[2] A.L. Solovjov, L.V. Omelchenko et al., Current Applied Physics 16, 931-938 (2016).

P05

High field study of UTe_3

Tetiana Haidamak[1], Michal Vališka[1], Andrej Cabala[1], Vladimir Sechvský[1], Yurii Skourski[2], Marc Uhlarz[2]

[1]Charles University, Faculty of Mathematics and Physics, Department of Condensed Matter Physics, Ke Karlovu 5, Prague, Czech Republic
[2]Hochfeld-Magnetlabor Dresden (HLD-EMFL), Helmholtz-Zentrum Dresden-Rossendorf, 01328, Dresden, Germany

UTe_3 is one of the representatives of binary uranium chalcogenides UT_x (T = S,Se,Te). Large single crystals of this compound were grown by the chemical vapor transport method. It crystalizes in the monoclinic structure of the $ZrSe_3$ type.

The single crystals of UTe_3 can be easily exfoliated and peel into layers confirming the presence of the Van der Waals bonds between the chalcogenide layers along the *c*-axis inside the unit cell.

Our heat capacity measurements confirmed that UTe_3 is an antiferromagnet with T_N = 5 K [1]. Its electrical resistivity increases exponentially with decreasing temperature followed by a sudden drop at 10 K.

Our high-field magnetization measurements up to 60 T revealed a metamagnetic transition at 20 T for the field applied along the *a**-axis.

[1] H. Noel, Journal of the Less Common Metals 121, 265-270 (1986).

P06

Robust pressure effects on magnetic orders in $NiBr_2$

Parvez Ahmed Qureshi[1], Jiří Prchal[1], Krishna Kumar Pokhrel[1], Subhasmita Ray[1], Petr Doležal[1], Sergui Arapen[2], Karel Carva[1], Vladimir Sechovsky[1], Jiri Pospisil[1]

[1]Department of Condensed Matter Physics, Charles University, Prague, Czech Republic
[2]IT4Innovations National Supercomputing Center, VSB - Technical University of Ostrava, Ostrava, Czech Republic

$NiBr_2$ is a van der Waals multiferroic material that crystallizes in the $CdCl_2$ structure type, featuring a frustrated triangular lattice of Ni^{2+} ions. At ambient pressure, it undergoes two successive magnetic transitions to a collinear in-plane antiferromagnetic (AFM) state that emerges at T_{N1} = 44 K, followed by an order-to-order transition at T_{N2} = 23 K into an incommensurate helical AFM phase. In the helical phase, multiferroicity arises due to spin-lattice coupling and Dzyaloshinskii-Moriya (DMI) interactions.

We present a study of the pressure-driven magnetism in $NiBr_2$ using AC magnetic susceptibility measurements up to 3 GPa complemented by first-principles calculations and Monte Carlo simulations. Our results reveal pressure stabilization of the collinear AFM phase with rapidly increasing T_{N1} up to ~100 K at 3 GPa. In contrast, the helical antiferromagnet phase carrying the multiferroicity is instantly suppressed at a critical pressure p_c of ~1 GPa. This transition signifies a pressure-induced enhancement in the competition between the strength of direct second-nearest-neighbor interlayer exchange interaction ($J_{2\perp}$) and intralayer frustration. The dominance of $J_{2\perp}$ under increasing pressure suppresses helical spin order, favoring a purely antiferromagnetic ground state, as confirmed by Monte Carlo simulations.

To probe the interplay between magnetism and lattice effects, we performed temperature dependent X-ray diffraction (3–300 K). We observed distinct changes in the a (a = b) and c lattice parameters, with the c-axis showing a sharp shift at T_{N1} and T_{N2}, directly linked to the magnetic transitions. This highlights strong magneto-elastic coupling, where magnetic fluctuations influence the lattice structure across both magnetic transitions.

Our findings highlight the role of pressure-driven exchange anisotropy in tuning the phase diagram of $NiBr_2$. These results position $NiBr_2$ as a promising platform for pressure-controlled quantum magnetism, offering insights into quantum criticality and emergent phases in low-dimensional van der Waals magnets.

P07

Search for new *RE*$AgBi_2$ compounds

Ivanna Arseniuk[1,2], Nazar Zaremba[1], Mitja Krnel[1], Andreas Leithe-Jasper[1], Yuri Prots[1], Yuri Grin[1], Bogdan Stelmakhovych[2], Eteri Svanidze[1]

[1]Max Plank Institute for Chemical Physics of Solids, Dresden, Germany
[2]Ivan Franko National University of Lviv, Lviv, Ukraine

The physical properties of rare earth (*RE*)-silver-bismuth and antimony-based materials have previously attracted a considerable amount of attention. In particular, the recent studies on Ce analogues found that all three compounds order antiferromagnetically, $CeNiBi_2$ below T_N=4.7 K [1], $CeCuBi_2$ below T_N=11.3 K [1], and $CeAgBi_2$ below T_N=6.4 K [2]. The gold-based analogues, namely $CeAuBi_2$, $PrAuBi_2$ and $NdAuBi_2$, also exhibit antiferromagnetic ordering, with both the Néel temperatures and magnetic anisotropy decreasing within the Ce–Pr–Nd series [3]. Other rare-earth-based isostructural compounds *RE*$AgBi_2$ (*RE* = La–Nd, Sm, Gd) were also investigated previously [4]. The existence of Dirac fermions in the quasi-two-dimensional CEF system $PrAgBi_2$ has been proposed [5]. Given the diversity of known systems, in this work we investigate whether other isostructural *RE*$AgBi_2$ systems can be stabilized.

[1] A. Thamizhavel et al., J. Phys. Soc. Jpn., 72, 2632–2639 (2003).
[2] S. M. Thomas et al., Physical Review B 93, 075149 (2016).
[3] E. M. Seibel et al., J. Solid State Chem., 230, 318–324 (2015).
[4] C. Petrovic et al., J. Magn. Magn. Mater., 261, 210–221 (2003).
[5] S. Malick et al., Physical Review B 111, 045144 (2025).

P08

Enhancing Fission Track Analysis for Nuclear Forensics: Image Processing Automation and Aerogel Integration

Rami Babayew[1,2], Yaacov Yehuda-Zada[1,2], Galit Bar[3], Noam Elgad[1,2], Mark Last[4], Jan Lorincik[5], Itzhak Orion[2], Shay Dadon[1], Aryeh Weiss[6], Galit Katarivas Levy[7], Itzhak Halevy[2]

[1]Engineering Department, Nuclear Research Center Negev, Beer-Sheva, Israel
[2]Unit of Nuclear Engineering, Faculty of Engineering Sciences, Ben Gurion University, Beer-Sheva, Israel
[3]Department of Solid-State Physics, Soreq Nuclear Research Center, Yavne, Israel
[4]Department of Software and Information Systems Engineering, Ben Gurion University, Beer-Sheva, Israel
[5]Nuclear Fuel Cycle Department, Centre Řež, Hlavní 130, Řež 250 68, Husinec, Czech Republic
[6]Bar Ilan University, Ramat Gan P.O.B. 90000 5290002, Israel
[7]Dept. of Biomedical Engineering, Ben-Gurion University, Beer-Sheva, Israel

Fission Track Analysis (FTA) is a pivotal tool in nuclear forensics, enabling identification and characterization of nuclear materials by examining fission fragment tracks in Solid-State Nuclear Track Detectors (SSNTDs). This study enhances FTA precision by introducing a novel detector design integrating Aerogel material and advanced image processing developed in MATLAB. Literature shows each fissile isotope exhibits a unique fission product yield. We propose that beyond identifying fissile particles, FTA can also reveal isotopic characteristics based on fission track length distributions. Monte Carlo simulations performed using GEANT4 with the QGSP_BERT_HP physics list to model fission product trajectories. Synthetic fission track clusters were generated using the FTA TRAINER 2.4, overlaying simulated tracks onto real SSNTD backgrounds (36 pixels = 1 µm). These datasets supported the development and validation of image processing algorithms for pattern analysis and property reconstruction. We validated the algorithms using both synthetic datasets and real fission tracks from the IAEA314 reference material. Synthetic data enabled controlled development, while real images tested robustness under realistic conditions.

Our methodology includes:

1. Fission Site Calculation: Hough transform-based edge detection to identify track lines and intersections to estimate the fission site.
2. Fission Track Recognition & Length Analysis: A classical image processing pipeline—filtering, edge detection, morphology, thresholding, and feature extraction—for precise track identification.
3. Property Reconstruction: Geometric analysis of light and heavy track lengths to characterize materials

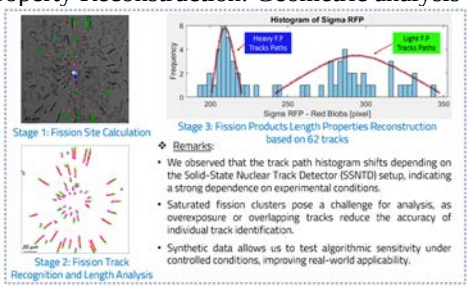

Analysis of U-235 100% Enrichment Synthetic Cluster

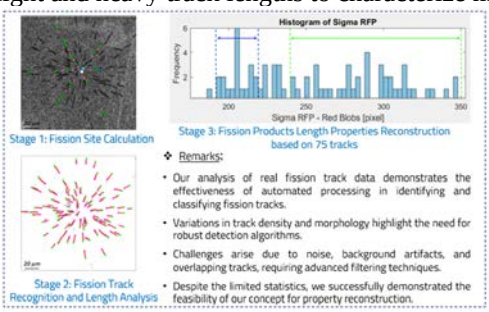

Analysis of U-235 Natural Enrichment Real Cluster

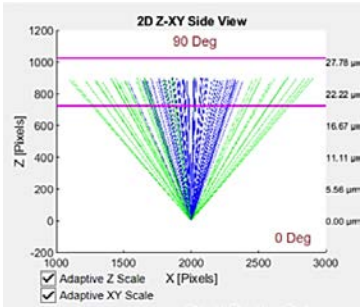

Side view of fission product flight path through 20 µm aerogel

Validation with real images confirmed robustness against noise, artifacts, and overlapping tracks.
To address limitations of traditional setups, we simulated Aerogel integration as a spacer material. Aerogel's low density and high transparency improved track separation and detection efficiency in simulations, showing high potential for future use.

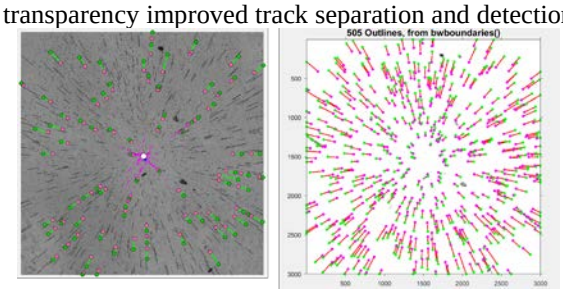

Processed images (SSNTD + Aerogel)

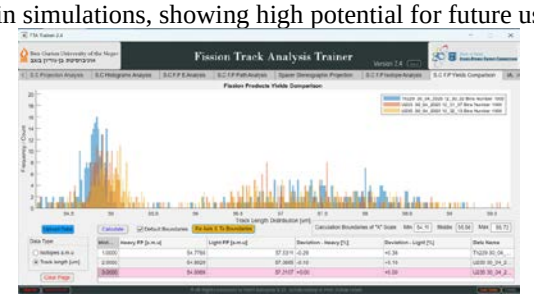

Histograms Comparison

Key Result:
Using GEANT4 datasets of Th-229, U-233, and U-235, image processing with Aerogel spacers revealed distinct histogram peak centers, supporting the concept of isotope differentiation through improved FTA.

P09

Influence of Hafnium on α-UH_3 Phase Stability and Magnetism in Uranium Hydrides

Shanmukh Veera Venkata Uday K Devanaboina[1], Oleksandra Koloskova[2], Ladislav Havela[1], Silvie Mašková-Černá[1,2]

[1]Department of Condensed Matter Physics, Faculty of Mathematics and Physics, Charles University, Prague, Czech Republic
[2]Institute of Physics (FZU), Czech Academy of Sciences, Prague, Czech Republic

Uranium hydride (UH_3) is one of the first known 5*f* materials to exhibit ferromagnetic ordering [1]. It exists in two different cubic modifications: a stable β-UH_3 phase (complex cubic with a = 664 pm), and a metastable α-UH_3 (*bcc* cubic with a = 414-416 pm). Our prime objective is to explore the role of Hafnium (Hf) in stabilizing the *bcc* α-UH_3 phase and examine its impact on the crystal lattice, magnetic, and transport properties.

In the present work, the alloys $U_{1-x}Hf_x$ with x = 0.10, 0.15, 0.30, and 0.40 were synthesized by arc-melting of pure elements (natural U-2N8, Hf-3N) in an Ar atmosphere. Subsequently, the alloys were hydrogenated by exposure to high pressure of H_2 gas (p = 100 bar) for 120 hours at ambient temperature. X-ray diffraction confirmed that 40 at.% of Hf alloying stabilizes the α-UH_3 phase, suppressing β-UH_3 formation at room temperature, and the determined lattice parameters of the stabilized α-UH_3 phase are in good agreement with the literature.

DC magnetization measurements reveal a ferromagnetic ground state with a Curie temperature (T_C) of 178 K, while increasing Hf concentration reduces spontaneous magnetization due to lattice dilution. The deviation from Curie-Weiss behavior, along with the downturn in the temperature-dependent inverse DC magnetic susceptibility and the peak formation above T_C in AC susceptibility measurements, supports the presence of magnetic inhomogeneities, likely due to the formation of short-range ferromagnetic clusters in the paramagnetic background – a hallmark of Griffiths-like phase behavior [2]. Further, the specific heat data reveal a magnetic entropy change (ΔS) of 2.5 J/mol·K near the Curie temperature, highlighting the complexity of magnetic interactions around T_C. These findings demonstrate the potential of Hf alloying to effectively tune both the structural stability and magnetic properties of uranium hydrides.

[1] Troc R., and Suski W., The discovery of the ferromagnetism in $U(H,D)_3$: 40 years later, J. Alloys Comp. 219, 1 (1995).
[2] Robert B. Griffiths, Nonanalytic Behavior Above the Critical Point in a Random Ising Ferromagnet, Phys. Rev. Lett. 23, 17 (1969).

P10

Sub-50mK adiabatic demagnetization refrigeration with frustrated Yb-oxide magnets in the PPMS.

Marvin Klinger, Jorginho Villar Guerrero, Anna Klinger, Tim Treu, Christian Heil, Paul Bittner, Anton Jesche, Philipp Gegenwart

EPVI, Center for Electronic Correlations and Magnetism, Institute of Physics, University of Augsburg, Augsburg, Germany

Accessing temperatures in the millikelvin (mK) regime is a prerequisite for quantum-matter research and in quantum technologies. Adiabatic demagnetization refrigeration (ADR) is a simple and sustainable alternative to ^{3}He/^{4}He dilution refrigeration. We have shown recently that geometrically frustrated rare earth oxides feature important advantages compared to the traditionally utilized hydrated paramagnetic salts for mK-ADR [1,2]. Refrigerants based on rare earth oxides exhibit high entropy density at low ordering temperatures compared to hydrated paramagnetic salts, allowing cooling to below 20 mK. Most importantly, they are chemically stable and can withstand high pressure and temperature cycling up to 600°C with no degradation of the refrigeration material, which is a significant advance over hydrated paramagnetic salts. Rare earth ADR materials are also compatible with ultra-high vacuum (UHV) conditions, and their mechanical manufacturability allows them to be pressed, cut, drilled, and milled for integration into various experimental setups.

We report the development of oxide-based customized ADR cooling platforms for use in the Quantum Design Physical Property Measurement System (PPMS). Temperatures below 20 mK were attained in standard PPMS Cryostats. Temperatures below 30 mK can be maintained for approximately 2.5 hours and below 100 mK for over 5 hours. Utilizing ADR allows for a cost competitive, high speed and easy to use mK measurement setup.

Our customized ADR inserts for the PPMS offer multiple experimental capabilities for electrical transport, magnetic susceptibility and heat capacity measurements. Additionally, they enable the use of piezo-strain tuning devices at mK temperatures. We present first experimental data utilizing these various probes.

[1] Y. Tokiwa et al., Commun. Mater. 2, 42 (2021).
[2] T. Treu et al., J. Phys. Condens. Matter 37, 013001 (2025).

P11

Magnetic structure and excitations in the antiferromagnet $Na_2BaMn(PO_4)_2$

David Svitak[1], Nikolaos Biniskos[2], Flaviano José dos Santos[3], Michal Stekiel[4], Bruce Normand[3], Karin Schmalzl[2], Andreas Lauchli[3], Petr Čermák[1]

[1] Charles University, Prague, Czech Republic
[2] ILL, Grenoble, France
[3] PSI, Villigen, Switzerland
[4] JCNS, Garching, Germany

The study of geometrically frustrated systems with antiferromagnetically (AFM) ordered spins has recently gained considerable attention for their exotic quantum magnetic properties. In order to explore effects related to quantum magnetism we investigate the triangular AFM $Na_2BaMn(PO_4)_2$, a compound with S=5/2.

By performing single crystal neutron diffraction and inelastic neutron scattering measurements we determine the magnetic structures and spin excitations, respectively, for magnetic fields applied in the basal plane and along the c-axis of the trigonal symmetry. At zero magnetic field the system undergoes two successive magnetic transitions at about 1.25 K (AFM2) and 1.1 K (AFM1), respectively. The out-of-plane incommensurate component *k* of the magnetic propagation vector (1/3, 1/3, *k*) exhibits a significant change in the two AFM phases and potentially indicates non-negligible interlayer couplings. Depending on the field direction, $Na_2BaMn(PO_4)_2$ undergoes several magnetic field induced transitions, which are accompanied by changes in the magnetic propagation vector, before reaching the spin polarized state. Combining neutron diffraction, low-temperature specific heat and dc magnetization we construct the temperature (T)-magnetic field (H) phase diagrams for the two field directions. Furthermore, with ab initio calculations and Monte Carlo simulations we extract the exchange interactions, anisotropy parameters and T-H phase diagrams.

The combined experimental and theoretical study reveals that $Na_2BaMn(PO_4)_2$ is a 2D-system with a very weak 3D coupling acting only as a "witness" for what is happening in two dimensions. The separation between the two zero-field transitions (AFM1 and AFM2) depends on XXZ nature of the anisotropy and on the 3D coupling, and the gap in the dispersion of the fully polarized phase depends on the XXZ, the single-ion anisotropies and on the magnetic field. Finally, we compare our results with the Co (with S=1/2) and Ni (with S=1) counterparts and we discuss their similarities and differences.

P12

LaueDB: A Dataset for Laue Patterns

Štěpán Venclík, Tomáš Červeň, Jan Kříž, David Sviták, Petr Čermák

Charles University, Prague, Czech Republic

Laue diffraction is a widely used technique for orienting single crystals and a routine procedure during sample preparation for many scientists. Over the years, a variety of software tools have been developed to assist in interpreting Laue patterns [1, 2]. Despite significant progress in image processing and pattern recognition, a robust and fully automated solution for indexing Laue patterns has yet to be achieved.

In recent years, **machine learning** has emerged as a promising approach to tackle this challenge [3]. However, the development and validation of more advanced algorithms are currently hindered by the lack of annotated experimental datasets. As a result, all training and testing are still conducted exclusively on synthetic data.

LaueDB aims to bridge this gap by creating a **dataset of oriented X-ray and neutron Laue patterns** that could serve as a training and evaluation dataset for both classical and machine learning approaches.

We plan to utilise the Automatic Laue Sample Aligner (ALSA) [4] to create the initial dataset, capturing a large number of patterns for each sample crystal, as well as collaborate with research infrastructures to develop a submission pipeline for patterns created during routine sample orientation. In addition, existing tools and algorithms for peak finding and Laue indexing will be compared.

[1] Esmeralda Laue Suite (https://code.ill.fr/scientific-software/esmeralda)
[2] Clip4 (https://clip4.sourceforge.net/)
[3] Purushottam Raj Purohit, R. R. P., Tardif, S., Castelnau, O., Eymery, J., Guinebretiere, R., Robach, O., Ors, T. & Micha, J.-S., J. Appl. Cryst. 55, 737-750 (2022).
[4] ALSA (https://charlesautomata.cz/alsa)

P13

Charles Automata: Physics laboratory automation

Tomáš Červeň, Jan Kříž, David Sviták, Štěpán Venclík, Petr Čermák

Charles University, Prague, Czech Republic

In recent years, there's been growing interest in turning research breakthroughs into real-world applications. But the reverse—**bringing industrial tools** like automation, robotics, and real-time control into the lab—can be just as transformative. These technologies, long used in industry, are now changing how scientific experiments are set up and run [1].

This talk **introduces a new suite of tools designed to streamline solid-state physics research**—especially sample preparation, which is often slow, manual, and error-prone. Automation offers better consistency, speed, and accuracy, which are increasingly important in today's data-heavy research world. Our previous work led to ALSA [2], a system for aligning monocrystals via Laue diffraction. Now, we're focused on making such technologies more accessible.

Enter **pSPARC** [3]: a compact, affordable **robotic system that automates sample handling** in both small labs and large facilities. It combines a high-precision Meca500 robot arm, an industrial camera, and a small computer, and connects seamlessly to lab instruments via the SeCoP protocol [4]. With features like automatic calibration, vision-based sample recognition, and plug-and-play usability, pSPARC is ready for researchers without robotics expertise.

By standardizing and speeding up sample handling, **pSPARC reduces downtime**—crucial in high-demand environments like synchrotrons or neutron beamlines. Its **open, modular design** also encourages **customization** and collaboration across the research community.

This presentation highlights how industrial-grade automation can empower scientists to work faster, smarter, and more reliably

[1] Szymanski, N.J., Rendy, B., Fei, Y. et al. Nature 624, 86–91 (2023).
[2] ALSA: Automatic Laue Sample Aligner (https://charlesautomata.cz/alsa).
[3] pSPARC: Portable Sample Aligner and Rapid Changer (https://charlesautomata.cz/psparc).
[4] Kiefer, Klaus, et al. J. Neutron Res. 21.3-4, 181-195 (2020).

P14

EuAl: synthesis, crystal structure and properties

Yurii Prots, Helge Rosner, Marcus Schmidt, Walter Schnelle, Yuri Grin

Max-Planck-Institut für Chemische Physik fester Stoffe, Dresden, Germany

The binary europium aluminide EuAl was synthesized from a mixture of the elements by arc melting and subsequent annealing at 570 °C in a closed tantalum container. According to results of a differential scanning calorimetry (DSC) and *in-situ* high-temperature synchrotron X-ray diffraction (ESRF, beamline ID22) the title compound decomposes peritectically at 630 °C. The crystal structure of EuAl (space group *Pmmn*, a = 5.806 Å, b = 9.652 Å, c = 10.088 Å) represents an unique atomic arrangement because other members of the *R*Al series (*R* - rare earth) crystallize either in CeAl (space group *Cmcm*) or in DyAl structure type (space group *Pbcm*) for La-Pr and Pr-Lu aluminides, respectively (for Pr both modifications exist). The significant deviation from the Vegard's rule of the unit cell volume normalized per formula unit clearly indicates a presence of Eu^{2+} in the reported compound. In the crystal structure of EuAl aluminium atoms are condensed into trigonal bipyramides (d(Al-Al) = 2.64-2.75 Å), which are interconnected (d(Al-Al) = 2.78 Å) into infinite chains along [100]. The chains are separated by europium species.

Transport and magnetic measurements at ambient conditions show that EuAl is a metallic system that undergoes magnetic ordering at about 70 K. The transition is accompanied by a strong drop (after a slight upturn) in the resistivity caused by the suppression of strong magnetic fluctuations. The effective local magnetic moment at high temperatures from a Curie-Weiss fit to the susceptibility yields a value of 8.15 μ_B per Eu (in average, since individual assignment of the moments is not possible from this measurements), demonstrating that all Eu sites are in a divalent state at ambient conditions. As can be concluded from the low temperature synchrotron diffraction (beamline ID22 at ESRF), the effects observed in the physical properties curves coincide with the anisotopic changes of the lattice parameters starting at the same temperature region.

Density functional calculations performed for EuAl yield a stepwise transition for a divalent to a trivalent state for the three different Eu sites, caused by their rather different local environment. The transition pressures are predicted between about 4 and 8 GPa. Due to the strong influence of quantum fluctuations a renormalization of the transition pressures or even just a single transition caused by strong coupling of the transition to the valence electrons and the lattice is expected.

P15

Taming Mosaicity with Robotics and AI: The Automatic Laue Sample Aligner (ALSA)

Jan Kříž, David Sviták, Tomáš Červeň, Štěpán Venclík, Petr Čermák

Charles University, Prague, Czech Republic

Inelastic neutron scattering is an indispensable tool for probing dynamic processes and excitations in crystalline materials, yet its efficiency is often hampered by low scattered flux from small samples. The Automatic Laue Sample Aligner (ALSA) [1] addresses this by automating the coalignment of single crystals: a process traditionally performed manually, which is time consuming and prone to variability. ALSA integrates a compact six axis Meca500 robotic arm [2], computer vision algorithms, and advanced control software to position crystals with high repeatability.

First, in collaboration with Karla Štěpánová's team from CTU's CIIRC, we are refining ALSA's computer vision pipeline beyond its current scope of achieving mosaicity of 1.5° on opaque crystal samples, as proven by trial demonstrations with a flux-grown Na2BaMn(PO4)2 [3] samples and verified by an OrientExpress [4] and IN12 triple axis cold neutron diffractometer [5] at ILL. Our main focus is optimizing functionality for transparent, colored and geometrically intricate crystals. Second, we are using CYTOP™ amorphous fluoropolymer coating [6] for its hydrogen-free composition, aiming to minimize neutron-scattering background [7]. Third, our NICOS integration now equips the native Meca500 controller with full collision avoidance and safety logic. A machine learning driven Laue pattern solver is under development to further streamline alignment workflows.

These hardware and software advancements promise to broaden ALSA's applicability across diverse sample types and significantly boost throughput, precision, and reproducibility in crystal coalignment for neutron experiments.

[1] https://charlesautomata.cz/alsa
[2] https://www.mecademic.com/meca500-industrial-robot-arm/
[3] Kim, Jaewook, et al. Journal of Physics: Condensed Matter 34.47, 475803 (2022).
[4] Ouladdiaf, B., et al. "Neutron Laue on OrientExpress," Physica B: Condensed Matter 385, 1052–1054 (2006).
[5] Schmalzl, Karin, et al. Nuclear Instruments and Methods in Physics Research Section A: Accelerators, Spectrometers, Detectors and Associated Equipment 819, 89-98 (2016).
[6] AGC Chemicals. CYTOP™ Amorphous Fluoropolymer Coatings Product Sheet.
[7] Rule, K. C., Mole, R. A., & Yu, D. "Which glue to choose? A neutron scattering study of various adhesive materials and their effect on background scattering," Journal of Applied Crystallography 51, 1766–1772 (2018).

P16

Crystal growth of unconventional superconductor UTe_2 and other U-Te intermetallics

Andrej Cabala, Michal Vališka, Jiří Pospíšil

Charles University, Faculty of Mathematics and Physics, Department of Condensed Matter Physics, Prague, Czech Republic

Uranium ditelluride (UTe_2) has attracted significant attention due to its unconventional superconducting properties. However, to reliably synthesize high-quality single crystals samples remains a major challenge, particularly in achieving consistent superconducting transition temperatures (T_s) and high residual resistivity ratio (RRR) values, both of which are essential for advanced physical property measurements. We systematically explored both the chemical vapor transport (CVT) and molten salt flux (MSF) methods, optimizing growth conditions and temperature profiles. Through our efforts the MSF method has shown a great promise in overcoming these difficulties. These efforts resulted in the reproducible preparation of UTe_2 single crystals with T_s slightly above 2 K and RRR values in the several hundreds, which is among the highest reported worldwide.

In parallel, we initiated growth studies on U_2Te_5, compound with structural similarities in form of layers of UTe_2 within a monoclinic van der Waals framework. Growth of U_2Te_5 comes with its own challenges, the primary difficulty lies in its close compositional proximity to another van der Waals compound UTe_3, which often forms preferentially under similar CVT conditions. We are currently refining the growth parameters to suppress the formation of UTe_3 and stabilize U_2Te_5. These efforts have also, somewhat unexpectedly, led to optimized growth recipes for high-quality UTe_3 crystals, opening new avenues for its systematic study.

This work was supported by the Czech Science Foundation under the grant # 25-16339S.

P17

Magnetism of $NdMn_{1-x}Ti_xO_3$ system

Matúš Mihalik[1], Magdalena Fitta[2], Krzysztof Siemek[2], Kamila Komędera[3], Jozef Polčák[4], Kornel Csach[1], Marian Mihalik[1]

[1]Institute of Experimental Physics Slovak Academy of Sciences, Košice, Slovakia
[2]Institute of Nuclear Physics Polish Academy of Sciences, Krakow, Poland
[3]WFIiS, AGH, Krakow, Poland
[4]CEITEC Brno University of Technology, Brno, Czech Republic

$NdMn_{1-x}Ti_xO_{3+\delta}$ ($0 \leq x \leq 1$) samples were prepared by a floating zone method in a mirror furnace, the crystal structure is orthorhombic, space group *Pnma*. XRPD results show that single-phase $NdMn_{1-x}Ti_xO_{3+\delta}$ compounds can be prepared by floating zone method in concentration range $0 \leq x \leq 0.3$. The EDX maps for $x = 0.6$ and $x = 0.8$ showed that the concentration of Mn and Ti ions varies. The evolution of the pseudo-cubic parameters shows two distinct regimes: $a_{pc} > c_{pc} > b_{pc}$ regime for $x < 0.3$ which is typical for perovskite structures were besides tilting of the octahedrons, cooperative Jahn-Teller distortion exists; and $a_{pc} > b_{pc} > c_{pc}$ for $x = 0.3$ and $x = 0.4$ where the distortion of the crystal lattice is driven mostly by the tilting of the octahedrons. XPS spectra show only the presence of Nd, Mn, Ti, O and C atoms and the detailed analysis of characteristic peaks for all elements was performed. Positron annihilation techniques revealed that only one positron lifetime $\tau_1 = 183.3$ ps exists in the case of $NdMnO_{3+\delta}$ as prepared sample. This result differs from the previous reports on similar compounds. The existence of only τ_1 component in the case of $NdMnO_{3+\delta}$ as prepared sample points to very high quality of the prepared material. The decrease of τ_1 and shifting the 95 % of intensity to τ_2 component for $NdMnO_{3+\delta}$ annealed sample indicate that practically all V_O vacancies have disappeared on the expenses of V_{Nd} or V_{Nd-O} vacancies. TG cycle shows that mass increases at temperatures higher than 740 °C for $x = 0.1$ and 0.2, or at temperatures higher than 700 °C for $x = 0.3$ substitution. Then, the mass passes through maximum at 1025 °C; 1026 °C and 1050 °C for $x = 0.1$; 0.2 and 0.3; respectively and decreases with increasing temperature due to reaching the dynamical equilibrium with the atmosphere. During cooling, dynamic equilibrium occurs at 1150 °C and then the mass increases up to 800 °C. Heat capacity measurements show broadening of lambda peak at phase transition with Ti-substitution. Compensation point was not observed on $NdMnO_{3+\delta}$ as prepared sample, but annealing resulted in one compensation point on ZFC curve, but 2 compensation points on FC curve. Magnetic properties of samples with Ti are more affected by atmosphere preparation/annealing post-processing than Mn ions. The shift of δ in the order of 10^{-2} for $NdMnO_{3+\delta}$ yields to the shift of T_N by -1.1 K and the shift of in the order of 10^{-1} for $NdMn_{0.9}Ti_{0.1}O_{3+\delta}$ yields to the shift of T_N by +1.1 K.

LIST OF PARTICIPANTS

Andreev Alexandr

Arseniuk Ivanna

Avila Miguel Geronimo

Cabala Andrej

Carva Karel

Custers Jeroen

Čermák Petr

Černá (Mašková) Silvie

Červeň Tomáš

Devanaboina Shanmukh V.V.U.K.

Evren Özlem

Fidrysiak Maciej

Gegenwart Philipp

Ghihor Anamaria

Haidamak Tetiana

Halevy Itzhak

Havela Ladislav

Honda Fuminori

Kancko Andrej

Kang Jeongsoo

Karychort Oksana

Klinger Marvin

Knapp Jan

Knappová Petra

Kolorenč Jindřich

Krnel Mitja

Kříž Jan

Kumar Sonu

Kuterba Piotr

Legut Dominik

Levy Galit Katarivas

Malick Sudip

Metoki Naoto

Mihalik Marian

Min Byung Il

Nixon Rachel

Pokhrel Krishna Kumar

Prots Yurii

Qureshi Parvez Ahmed

Radwanski Ryszard

Riseborough Peter

Sechovský Štěpán

Sourd Jérémy

Spałek Józef

Svanidze Eteri

Svitak David

Tkáč Vladimír

Tobin James

Tokiwa Yoshifumi

Treu Tim

Vališka Michal

Venclík Štěpán

Vyalikh Denis

Wilhelm Fabrice

Zaremba Nazar

Zwicknagl Gertrud